NUWC-NPT Technical Report 10,771
12 December 1994

Molecular Modeling: An Approach for the Study of Piezoelectric Polymers

George J. Kavarnos
Submarine Sonar Department

Naval Undersea Warfare Center Division
Newport, Rhode Island

PREFACE

The work described in this report was sponsored by the Naval Undersea Warfare Center's Independent Research (IR) Program, as Project No. A11800, entitled "Use of Molecular Modeling for Improved Copolymer Wide-Aperture Array." The IR program is funded by the Office of Naval Research; the NUWC program manager is Dr. Kenneth M. Lima (Code 102).

The technical reviewer for this report was Dr. Harold Robinson (Code 3111).

The author acknowledges with deep gratitude the support of Dr. Kenneth Lima, IR Program Manager, Naval Undersea Warfare Center Division Newport, the assistance of Dr. Robert Holman (Western Kentucky University), and the encouragement of Jan Lindberg (Code 213) and James Powers (Code 2131).

Reviewed and Approved: 12 December 1994

R. J. Martin
Head, Submarine Sonar Department

REPORT DOCUMENTATION PAGE

Form Approved
OMB No. 0704-0188

1. AGENCY USE ONLY (Leave Blank)	2. REPORT DATE	3. REPORT TYPE AND DATES COVERED
	12 December 1994	Final

4. TITLE AND SUBTITLE

Molecular Modeling: An Approach for the Study of Piezoelectric Polymers

5. FUNDING NUMBERS

PR A11800

6. AUTHOR(S)

George J. Kavarnos

7. PERFORMING ORGANIZATION NAME(S) AND ADDRESS(ES)

Naval Undersea Warfare Center Detachment
39 Smith Street
New London, Connecticut 06320-5594

8. PERFORMING ORGANIZATION REPORT NUMBER

TR 10,771

9. SPONSORING/MONITORING AGENCY NAME(S) AND ADDRESS(ES)

Naval Undersea Warfare Center Division
1176 Howell Street
Newport, Rhode Island 02841-5594

10. SPONSORING/MONITORING AGENCY REPORT NUMBER

11. SUPPLEMENTARY NOTES

12a. DISTRIBUTION/AVAILABILITY STATEMENT

Approved for public release; distribution is unlimited.

12b. DISTRIBUTION CODE

13. ABSTRACT (Maximum 200 words)

This report describes the use of molecular modeling and computational chemistry techniques to investigate and tailor the piezoelectric properties of polyvinylidene fluoride (PVDF) and its copolymer with trifluoroethylene (PVDF-TrFE) for underwater hydrophone and acoustic projector applications. The effect of changing the ratios of vinylidene fluoride and trifluoroethylene monomers was studied using a combination of semiempirical molecular orbital theory, molecular mechanics, and crystal packing approaches. Molecular mechanics calculations on model end-capped polymer chains show that the *tgtg'* conformation of PVDF is 0.5 to 0.7 kcal/mol more stable than the all-*trans* formation but that for copolymer compositions less than 90 mol% vinylidene fluoride (VDF), the all-*trans* conformation is favored. Crystal packing calculations confirm the stability of the *tgtg'* for PVDF and the all-*trans* for the copolymers. To calculate the elastic compliances of PVDF and copolymer unit cell crystals along the poling direction, the b-axes were deformed in small increments and the crystal packing energies of each deformed structure were calculated. This procedure was used to determine the elastic compliances, which were calculated to be 2.59×10^{-11} m^2/N for PVDF, 3.97×10^{-11} m^2/N for 75 mol% VDF copolymer, and 5.38×10^{-11} m^2/N for 50 mol% VDF copolymer. The $d_{33}{}^c$ constants of the unit cells were calculated to be –3.3 pC/N for PVDF, –4.0 pC/N for 75 mol% VDF copolymer, and –4.3 pC/N for 50 mol% VDF copolymer. Although these values are much lower than the experimental d_{33} constants of semicrystalline polymer, a procedure used to calculate the d_{33} constants of semicrystalline polymer yields d_{33} constants much more in agreement with the experimental values.

14. SUBJECT TERMS
Molecular Modeling
Piezoelectric Polymers
Piezoelectric Properties

15. NUMBER OF PAGES
46

16. PRICE CODE

17. SECURITY CLASSIFICATION OF REPORT	18. SECURITY CLASSIFICATION OF THIS PAGE	19. SECURITY CLASSIFICATION OF ABSTRACT	20. LIMITATION OF ABSTRACT
Unclassified	Unclassified	Unclassified	SAR

TABLE OF CONTENTS

LIST OF ILLUSTRATIONS

LIST OF TABLES

MOLECULAR MODELING: AN APPROACH FOR THE STUDY OF PIEZOELECTRIC POLYMERS

INTRODUCTION

The central theme of this report is to demonstrate how molecular modeling can be used to study, predict, and tailor the piezoelectric properties of semicrystalline polyvinylidene fluoride (PVDF) and its copolymer with trifluoroethylene P(VDF-TrFE). This is an application where molecular modeling has been successfully used to understand and improve the properties of piezoelectric polymers for active and passive sonar. PVDF and P(VDF-TrFE) are remarkably versatile polymers. PVDF consists of thousands of repeating monomeric units of vinylidene fluoride (VDF). Since this polymer is prepared from a single monomer, it is often referred to as a *homopolymer*. A schematic of PVDF is shown in figure 1 where "A" represents the VDF monomer. P(VDF-TrFE) is composed of vinylidene fluoride and trifluoroethylene (TrFE) monomers. These monomers can be arranged in varying ways leading to several possible structures. P(VDF-TrFE) is said to be a *random copolymer* since the distribution of its monomers is random. A possible arrangement is shown in figure 1 for "A" and "B" monomers. Since copolymer compositions may differ in their fluorine content, the properties of these compositions are determined by the relative ratios of the VDF and TrFE monomers.

Both PVDF and P(VDF-TrFE) can be processed into semicrystalline, nonpolar materials. When poled in a strong electric field, P(VDF-TrFE) is converted into a polar, piezoelectric material.[1] PVDF, however, must be stretched before it converts into its piezoelectric form. When mechanically stressed, piezoelectric PVDF and P(VDF-TrFE) generate an electric polarization; when electrically stressed, they undergo mechanical deformation.[2,3] The polarization of PVDF and P(VFE-TrFE) is due to a highly oriented alignment of the numerous carbon-fluorine dipoles along the direction of the electric field. The position of fluorine in the periodic table guarantees its strong electronegativity, which means that it can attract electrons from the neighboring carbon atom to which it is attached. This leads to the development of a carbon-fluorine dipole. The presence of fluorine also confers PVDF and P(VDF-TrFE) polymers with their remarkable properties including, for example, their hydrophobicity, water insolubility, stability to thermal and oxidative degradation, and resistance to fire, oil, and organic solvents.

Piezoelectric fluoropolymers offer several advantages when compared with traditional piezoelectric ceramics used in underwater sonar. Polymers are light, mechanically flexible, robust, conformal, and better acoustically-matched with water than conventional ceramics.[4] Because of these features, PVDF has been considered as

a passive hydrophone material for large aperture arrays on future submarines. P(VDF-TrFE) is a potential candidate for underwater acoustic projectors of broad bandwidth requiring stacks of thick electroded elements.[5] Since there is no requirement for mechanical stretching of the copolymer chains, solvent-cast or melted copolymer can be poured into molds, annealed to induce crystallization, and then poled.

At the outset of this project, the question of polymer composition emerges as an issue of central importance. For example, how do the mechanical, electrical, and thermal properties vary as a function of fluorine content? In the case of P(VDF-TrFE), what are the optimum compositions for piezoelectric performance? Can a predictive model be formulated to allow the transducer designer to select the most appropriate composition for a specific sonar application? The objective of this research was to use molecular modeling to gain deeper insight into the piezoelectric properties of PVDF and P(VDF-TrFE) and to develop a practical predictive framework to assist the transducer designer in selecting and tailoring the properties of various polymer compositions for underwater sonar transduction applications.

THEORY

THE MOLECULAR AND CRYSTAL STRUCTURES OF PVDF AND P(VDF-TrFE)

In this section, we describe briefly the structural characteristics of PVDF and P(VDF-TrFE). PVDF is synthesized by the polymerization of 1,1-difluoroethylene, or vinylidene fluoride.[6] The repeating monomer units have the formula $-CH_2-CF_2-$, where C, H, and F are the chemical symbols for the carbon, hydrogen, and fluorine atoms, respectively (figure 2). The carbon atoms are connected to one another by single bonds to form the polymer backbone. The hydrogen and fluorine atoms are each bonded to individual carbon atoms. The molecular formula of PVDF is often written as $(CH_2-CF_2)_n$, where n typically may range from about 30,000 to 80,000. The monomer units of PVDF can be linked as shown in figure 3 giving rise to two chain configurations. The CF_2 portion of the monomer is often referred to as the "head" and the CH_2 portion the "tail." The PVDF chain is composed largely of regular head-to-tail sequences. Most polymer compositions will have a small percentage of head-to-head or tail-to-tail defects.

P(VDF-TrFE) is synthesized from vinylidene fluoride and 1,1,2-trifluoroethylene.[6] The molecular structure of the copolymer is made up of $-CH_2-CF_2-$ and $-CHF-CF_2-$ monomer units (figure 2) connected to one another in a random fashion. The composition of a P(VDF-TrFE) copolymer is expressed in terms of the percent distribution of moles of VDF monomers, e. g., 75 mol% refers to a copolymer

in which the distribution of VDF and TrFE monomer units is 3:1.

In the melt or in solution, the polymer exists as numerous, long, spaghetti-like chains. The randomly coiled chains are constantly moving. These motions may consist of rotations about the numerous carbon-carbon single bonds that comprise the polymer backbone.[7] During cooling of the melt or during solvent evaporation, dynamical motions about the carbon-carbon single bonds lead to chain folding. The packing of the folded chains results in the formation of crystallites. The propensity of these polymer chains to pack into discrete crystal structures is related to the small van der Waals (vdW) radius of fluorine, which is only about 1.35 Å.[8] If the size of fluorine were smaller, let us say about the size of the hydrogen atom (1.2 Å), the fluoropolymers would behave like polyethylene and would not exhibit as many stable polymorphic structures (the structures of crystal polymers are referred to as polymorphs). The polymer would then tend to form only the most stable polymorph. Were the van der Waals radius of fluorine larger, the rotational barriers would be so great that interconversions between polymorphs would be restricted, i.e., the chain would stiffen. This is not the case with fluoropolymers where the barriers to rotations are not so high that transitions are prevented and not so low that only the most stable structure is always favored. In other words, the polymer can "lock" into structures not necessarily having the lowest energies.

The crystal structures of PVDF and P(VDF-TrFE) can be described as stacks of lamellae immersed in a sea of amorphous regions of disordered chain conformations (figure 4).[9,10] The lamellae are thin platelet-like structures about 100 Å thick and several microns broad.[11] The size of the lamellae is sensitive to crystallization conditions. A microscopic examination of the interlamellar regions reveals nonordered, isotropic chains connecting the crystallites.[12] The chains in the amorphous region can be entangled and knotted. Long loops can exit and enter the same crystallite. Some loops can even join adjacent lamellae. Thus, the polymers are complex, two phase, semicrystalline materials. This feature of PVDF and P(VDF-TrFE) polymers plays a profound role in their piezoelectric performance.

Although several polymorphs for PVDF and P(VDF-TrFE) have been identified, we will, for our purposes, consider only the polymorphs that play a pivotal role in their piezoelectricity, the α- and β-phases. Segments of the chain conformations for these polymorphs of PVDF are illustrated in figure 5. The conformational structures of P(VDF-TrFE) are similar. When PVDF crystallizes from the melt or solution and the polymer subsequently anneals, the chains pack preferentially into a crystalline polymorph called the α-phase.[9,13] During the annealing process, the mobility of the chains guarantees that they can pack into crystal cells.[14] In the α-phase, the sequential arrangement of the torsional or dihedral angles formed between neighboring C-F and C-H bonds as one looks along a single C-C bond is in the neighborhood of 60°, 180°, -60°, 180°, etc (the atoms forming a dihedral angle are connected to one another sequentially as illustrated in figure 6). For shorthand, we

write this as *tgtg'* where *t* refers to *trans* or 180°, and *g* or *gauche* is a 60° dihedral angle. The actual torsional angles along the backbone of polymer chain may deviate considerably from these "ideal" values. However, when we want to study the effects of changes in dihedral angles on chain properties, it is quite useful to compare the dihedral angles of the packed chain with those of the "ideal" chain. This gives us some clue concerning the magnitude of the deformation energies required to distort the chain from the "ideal" values. This loss in energy stabilization is usually compensated for by a great gain in crystal packing energy.[15] This is an important point to which we shall return below.

One of the salient features of the α-phase crystal is that it is nonpolar. Two α-phase chains pack into a unit cell such that the C-F dipoles normal to the chain axis cancel out. This can be visualized in figure 7, which displays a projection of the α-phase unit cell looking into the direction of the chain axis. When the α-phase is stretched mechanically, the chains undergo torsional motions and transform into a sequence of repeating 180° torsional angles. This is the β-phase, which is characterized by an all-*trans* conformation (figures 5 and 7). The C-F dipoles of the β-phase chain are aligned and pointed in the same direction. When two β-phase chains pack into an orthorhombic unit cell, the net result is that the unit cell acquires a net cell dipole moment, as shown in figure 7. When poled in an electric field, the individual unit cells collectively undergo reorientation. The oriented chains are now polarized and piezoelectric.

P(VDF-TrFE) is known to crystallize predominantly into a β-phase unit cell possessing monoclinic symmetry. The net polarization of a unit cell containing the $CHF\text{-}CF_2$ is less than that of $CF_2\text{-}CH_2$ since the former has a C-F dipole on CHF which opposes the direction of the dipole on CF_2. This loss in polarization might be expected to result in the loss of piezoelectricity, but this is not so as shall be demonstrated in a later section. We shall show that piezoelectricity is influenced not only by the polarization of the crystalline phase but also by the mechanical compliance of both the crystalline and amorphous phases.[16]

The fact that P(VDF-TrFE) can crystallize into the polar form without mechanical stretching is one of the great advantages of the copolymer. However, when one considers the range of possible P(VDF-TrFE) compositions, it is not obvious what ratios of VDF and TrFE are a prerequisite for the direct crystallization into the β-phase. This question was examined from the perspective of molecular modeling. Before describing this study, we shall provide a short background on molecular modeling.

MOLECULAR MODELING

One of the objectives of molecular modeling is to determine the optimum geometry and properties of a molecule, molecular fragment, or crystal. Many useful properties of the molecule or crystal can be extracted with knowledge of the optimized geometry. The ability to predict the properties of solid-state materials using molecular modeling techniques has made it possible for material scientists to tailor the macroscopic properties of these materials and to fine-tune the processing conditions used to engineer these materials for specific applications. Traditionally, molecular modeling was used by chemists to study the properties of simple organic and inorganic molecules or to predict the course of chemical reactions. The computational approaches can range from classical, Newtonian force fields that treat molecules as "ball and stick" structures to quantum mechanical calculations that consider electronic interactions. The approach depends on the nature of the application as well as the size of the molecular structure. One can, for example, solve the Schrödinger equation for the hydrogen molecule with a simple calculator. But for larger molecular systems such as polymers, adequate computer resources are essential to calculate certain properties. With the advent of powerful computer programs and resources, it has become possible to extend the classical and quantum mechanical algorithms that were originally intended for small molecules to huge solid-state systems consisting of millions of atoms. However, even with large computers, performing calculations on solid-state molecular structures is still a daunting task. A far better approach is to consider fragments of the solid-state.[17] The task can be made even more manageable if the solid-state consists of periodic or repeating units such as a polymer.[18] By focusing on the properties of the crystal unit cell and the dimensionality of the crystal, one can draw conclusions about the behavior and characteristics of the macroscopic material.[19]

The approach in this study was to perform geometry optimization on a small segment of a polymer chain.[20] Geometry optimization and assignment of charges were carried out using semiempirical molecular orbital theory. The optimized structure was then packed into a crystal cell. Crystal packing calculations were then carried out on the relaxed crystal unit cell using intermolecular analytical functions. In calculating the energies of large, single, end-capped polymer chains, we used molecular mechanics for economical reasons since this method demands fewer computer resources than the more computationally intensive semiempirical molecular orbital theory. Molecular mechanics was also used to calculate the net dipole moments of crystal unit cells.

MOLECULAR MECHANICS

In the molecular mechanics approach, the atoms comprising the molecule are visualized as hard spheres and the bonds linking the atoms as springs. The energy

of the molecule depends on the interatomic distances, bond angles, conformations, and relative orientation of dipoles. Each interaction can be described by an analytical function called a *force field*. From the geometry of the equilibrium structure, it is possible to deduce certain molecular and macroscopic properties. In the subsequent discussion, it will be useful for the reader to refer to figure 6, which illustrates the important geometrical features of a molecule including the bond length, bond angle, torsional or dihedral angle, and interatomic distance.

The intramolecular energy, E_{intra}, of any molecule or molecular fragment can be written as[21]

$$E_{intra}=E_s+E_\theta+E_{sb}+E_{vdW}+E_{tor}+E_\mu, \tag{1}$$

where E_s is the bond length deformation potential, E_θ is the bond angle deformation potential, E_{sb} is the stretch-bend potential, E_{vdW} is the van der Waals interaction potential, E_{tor} is the torsional or dihedral potential, and E_μ is the dipole interaction potential. Each term in equation (1) represents a component of the total force field of the molecule or molecular fragment. The force field due to the sum of all changes in bond lengths, for example, can be described by Hooke's law:

$$E_s=\sum \frac{k_s}{2}(l-l_o)^2, \tag{2}$$

where l is the bond length between two atoms, l_o is the equilibrium, or most stable, bond length, and k_s is the force constant when the bond length is deformed or displaced from the lowest energy position. The bond-length parameters used in the molecular mechanics program for this study are listed in table 1.[22,23]

For bond-angle deformations, the potential is

$$E_\theta=\sum \frac{k_\theta}{2}(\theta-\theta_o)^2, \tag{3}$$

where θ is the bond angle, θ_o is the equilibrium bond angle, and k_θ is the bond angle deformation force constant. The relevant parameters are shown in table 2.[22,23] Stretch-angle bending cross terms refer to the coupling between bond stretching and angle bending. These motions are accommodated by the expression given below:

$$E_{sb}=\sum k_{sb}(\theta-\theta_o)_{ijk}[(l-l_o)_{ik}+(l-l_o)_{jk}], \quad (4)$$

where k_{sb} is the stretch-bending force constant. The stretch-bending force constants are 0.120 mdyn/Å for C-C-C, C-C-F, and F-C-F angles; and 0.090 mdyn/Å for C-C-H and H-C-F angles. No force constants are defined for H-C-H.

The analytical function for torsional or periodic rotations about single bonds is

$$E_{tor}=\sum [\frac{V_1}{2}(1+\cos\phi)+\frac{V_2}{2}(1-cos2\phi)+\frac{V_3}{2}(1+\cos3\phi)], \quad (5)$$

where φ is the dihedral angle and V_1, V_2, V_3 are force constants for individual torsional barriers (table 3).[24]

The sum of non-bonded van der Waals interactions, i.e., those weak forces arising from interactions between nonbonded atoms on the same molecule, can be described by

$$E_{vdW}=\sum \epsilon_{ij}[2.9x10^5\exp(-12.5\rho_{ij})-2.25\rho_{ij}^{-6}], \quad (6)$$

where ε_{ij} is defined by

$$\epsilon_{ij}=\sqrt{\epsilon_i \epsilon_j}, \tag{7}$$

and ε_i and ε_j are referred to as "hardness" parameters. The following expression defines ρ_{ij}:

$$\rho_{ij}=\frac{R_{ij}}{r_{ij}}, \tag{8}$$

where R_{ij} is the nonbonded distance between the interacting atoms, and r_{ij} is the sum of the individual van der Waals radii of atoms i and j ($r_{ij} = r_j + r_j$). When r_{ij} is less than 3.311, the following expression is used:

$$E_{vdW}=\sum \epsilon_{ij}\rho_{ij}^{-2}. \tag{9}$$

The nonbonded parameters used in equations (6) to (7) are summarized in table 4. When equation (9) is used for a C-H bond, ε and r are 0.046 and 3.340 Å, respectively.

The dipole-dipole interactions can be accommodated by the following equation:

$$E_{\mu}=\epsilon_s \sum \mu_i \mu_j \left[\frac{\cos\chi - 3\cos\alpha_i \cos\alpha_j}{R_{ij}^3}\right], \tag{10}$$

where μ_i and μ_j are the dipole moments of atoms i and j; ε_s is the dielectric constant assumed here to be 1.5; χ is the angle between two dipole vectors; and α_i and α_j are the angles that each of the two dipoles make with the vector separating them (figure 8).

The potential energy of an optimized geometry of a molecule or molecular

fragment must satisfy the equation

$$\frac{\partial V}{\partial r_i}=0, \tag{11}$$

where r_i represents a cartesian coordinate.[25] Typically, the coordinates of an X-ray diffraction structure are used as the starting or initial geometry. The first derivative of the potential energy with respect to the atomic coordinates is recorded as increments are added to those coordinates. This is accomplished by changing the positions of the atoms in tiny increments. Minimization proceeds in a direction of the negative gradient of the potential energy until equation (11) is satisfied.

The success of a molecular mechanics calculation depends on the selection of realistic force constants. These are generally obtained spectroscopically or by quantum mechanical calculations. An extensive listing of published force-field parameters is available.[26]

Geometry optimizations on end-capped polymers were carried out using the force fields described by equations (2) to (10). Calculations were performed using the HyperChem software on a 4D Silicon Graphics workstation. This package contains the mm+ force field, which is derived from the MM2 molecular mechanics software developed by Allinger.[27] MM2 is the 1977 version of molecular mechanics, which is available as program QCMP004 from the Quantum Chemistry Program Exchange at Indiana University.

SEMIEMPIRICAL QUANTUM MECHANICS

Since molecular mechanics does not explicitly consider effects of electrons, the accuracy of this methodology depends on the quality of the force fields and parameters for the atoms of interest. This is of no consequence if electronic interactions and bond-stretching are not important. To obtain "higher" quality results, it is desirable to consider the properties of the electrons and to solve the Schrödinger equation to obtain these properties. This procedure can be done with semiempirical quantum mechanics, which solves an approximate form of the Schrödinger equation, or by *ab initio* quantum mechanics, which does not use any experimental parameters to solve the Schrödinger equation. In the interest of economy and effciency, we chose the semiempirical approach for geometry optimization of small polymer fragments. The semiempirical theory was also used to calculate the tensile elastic moduli when

stretching polymer chains. This operation is discussed in a later section.

To treat electronic effects explicitly, we need to solve the Schrödinger equation for the molecular system of interest. In semiempirical methods, interactions within the nuclear core and nonvalence electrons are neglected. Overlap between valence electrons is handled by empirical functions.

Semiempirical methods produce approximate solutions to the Schrödinger equation:[28,29,30]

$$H\Psi(r)=E\Psi(r). \tag{12}$$

The molecular Hamiltonian, H, is a description of the particles of a system and $\Psi(\mathbf{r})$ is the wave function of the molecular system. The position of the particles of the system is designated by **r**. The molecular Hamiltonian is the sum of kinetic and potential energy terms:

$$H=T+V, \tag{13}$$

where T, the kinetic energy, is

$$T=\frac{-h^2}{8\pi^2}\sum_k \frac{1}{m_k}\nabla, \tag{14}$$

where m_k is the mass of the kth particle. The differential operator, ∇, is given by

$$\nabla=\frac{\partial}{\partial x}i+\frac{\partial}{\partial y}j+\frac{\partial}{\partial z}k, \tag{15}$$

where x, y, and z represent the position components of the particle. The potential

energy, V, is

$$V=-\sum_{i}^{e}\sum_{I}^{n}\left(\frac{Z_I e^2}{\Delta R_{iI}}\right)+\sum_{i}^{e}\sum_{j}^{e}\left(\frac{e^2}{\Delta R_{ij}}\right)+\sum_{I}^{n}\sum_{J}^{n}\left(\frac{Z_I Z_J e^2}{\Delta R_{IJ}}\right), \tag{16}$$

where ΔR_{ij} is the distance between two particles, Z is the atomic number of the nucleus, Ze is charge, and e and n are designations for electron and nucleus, respectively. The lower and upper case subscripts in equation (16) also refer to the electrons and nuclei, respectively. To simplify the problem, we employ the Born-Oppenheimer approximation, which allows us to treat the properties of nuclei and electrons separately. The Born-Oppenheimer approximation rests on the fact that nuclear motion is much slower than electronic motion, which is reasonable given that the mass of an electron is much lighter than the mass of the nucleus. Electronic motion, which can now be treated independently without considering the nuclear kinetic energy, is described by the electronic Hamiltonian

$$H_e=-\frac{1}{2}\sum_{i}^{e}\nabla-\sum_{i}^{e}\sum_{I}^{n}\left(\frac{Z_I}{|\vec{R}_I-\vec{r}_i|}\right)+\sum_{i}^{e}\sum_{j}^{e}\left(\frac{1}{|\vec{r}_i-\vec{r}_j|}\right)+\sum_{L}^{n}\sum_{J}^{n}\left(\frac{Z_I Z_J}{|\vec{R}_I-\vec{R}_J|}\right). \tag{17}$$

When the Schrödinger equation is solved using the electron Hamiltonian from equation (17), the energy obtained is the effective nuclear potential function describing the potential energy surface of the molecular system. It is important to note that Ψ must be normalized; that is, the total probability of finding the electron in space must be

$$\int_{-\infty}^{+\infty}|c\Psi|^2 dv=1, \tag{18}$$

where c is any constant and v is "space volume."

There are a number of simplying assumptions that must be employed. One of these is that the molecular orbital can be expressed as a linear combination of the

individual atomic orbitals:

$$\Psi = \sum c_{\lambda i}\phi_{\lambda}, \tag{19}$$

where ϕ_{λ} is an atomic orbital and $c_{\lambda i}$ is the molecular orbital expansion coefficient for the atomic orbital. By convention, we designate Roman subscripts for molecular orbitals and Greek subscripts for atomic orbitals. The molecular orbital expansion coefficients are solved by using the variational principle. This is because the Hartree-Fock method is based on the relationship,

$$E(\Xi) > E(\Psi), \tag{20}$$

i.e., the minimum energy, E(Ξ), will still be larger than the exact energy, E(Ψ).

In the Hartree-Fock method, the Self-Consistent Field (SCF) approach is employed where the position of each electron is guessed as well as its average potential in the field of other electrons. The Schrödinger equation is solved to obtain a new "guess" of the positions. This procedure is repeated until the wavefunction of each electron is "consistent" with the fields of all electrons. When solving for the coefficients in equation (19), the energy of the wavefunction must be minimized. To solve for the molecular orbitals, we must determine the coefficients of the atomic orbitals. We do this step using the Roothaan-Hall secular equation:

$$\sum_{1}^{N} (F_{\mu\nu} - \epsilon_i S_{\mu\nu}) c_{\nu i} = 0, \tag{21}$$

where ε_i is the spin-free one-electron orbital energy of an orbital (μ = 1, 2, ···, N); S is the matrix representing overlap between orbitals, i.e.,

$$S_{\mu\nu} = \langle \varphi_{\mu}(1) | \varphi_{\nu}(1) \rangle, \tag{22}$$

and F is the Fock matrix,

$$F_{\mu\nu} = H_{\mu\nu} + \sum_{\lambda}^{N} \sum_{\sigma}^{N} P_{\lambda\sigma} [\langle \mu\nu | \lambda\sigma \rangle - 1/2 \langle \mu\lambda | \nu\sigma \rangle], \tag{23}$$

where $H_{\mu\nu}$ is a matrix of the energy of a single electron in the field of bare nuclei.

The term $\langle \mu\nu | \lambda\sigma \rangle$ is a two-center two-electron integral between a pair of atoms; thus,

$$\langle \mu\nu | \lambda\sigma \rangle = \int \varphi_\mu(1)\varphi_\nu(1)\left(\frac{1}{r_{12}}\right)\varphi_\lambda(2)\varphi_\sigma(2)d\tau, \tag{24}$$

where $P_{\lambda\sigma}$ is the density matrix, which can be written as

$$P_{\lambda\sigma} = 2\sum_{i=1}^{occupied} c^*_{\lambda i} c_{\sigma i}. \tag{25}$$

Solving equation (21) is done by matrix diagonalization. This leads to the coefficients used to describe the atomic orbitals in equation (19). The total electronic energy in equation (21) is, therefore, defined as

$$E = \frac{1}{2}P(H+F). \tag{26}$$

The details of matrix diagonalization and the functions used to calculate molecular properties such as atomic charge are outside the scope of this report. The interested reader may want to consult one of the excellent reviews or books referenced in this section.

MOPAC is currently the most popular general-purpose semiempirical molecular orbital program.[31] This program represents the collective effort of numerous groups who over the years have implemented a variety of semiempirical methods. In MOPAC, a starting geometry must be specified. As in the case of classical methods, geometry optimization is carried out with derivatives with respect to the coordinates. In each iteration, the heat of formation is calculated. When there is no further change in energy, geometry optimization stops. In this work, MOPAC was used to minimize the polymer segments which were packed into crystal cells.[32] This was done to accommodate the effects of the atomic charges on the crystal packing energies.

CRYSTAL PACKING CALCULATIONS

The structure obtained after minimization of a chain segment is used to calculate the total potential energies and the dipole moments of individual unit cells. To perform this operation, it is first necessary to "pack" the individual chain segments into appropriate unit cells. "Packing" refers to the alignment and arrangement of the

chain segments into a crystal cell. The lattice dimensions and angles are altered to minimize repulsive electrostatic and vdW interactions between atoms on neighboring chains and to maximize attractive electrostatic and vdW interactions. Intermolecular electrostatic interactions are accommodated by the sum of individual interactions between charged atoms on neighboring chains:[33]

$$E_e = \sum \frac{q_i q_j}{R_{ij}}, \tag{27}$$

where E_e is the coulombic energy, q_i and q_j are the charges on atoms i and j. Atoms possessing the same charge will repel one another, whereas those with opposite charges attract. Intermolecular van der Waals interactions are calculated using the potential shown below:[33]

$$E_{vdW}(crystal) = \sum \epsilon_{ij}[\rho_{ij}^{-12} - 2\rho_{ij}^{-6}]. \tag{28}$$

One usually starts with the structure of a crystal whose dimensions have been determined by x-ray crystallography. Once the chain segments are packed within the cell, the interactions between them are minimized by changing the lattice dimensions and angles in tiny increments. Eventually, a relaxed crystal structure and its intermolecular energy are obtained. The geometry of this structure should not deviate significantly from the experimental x-ray structure. The crystal packing calculations described in this report were performed using the CERIUS Version 3.1 software provided by Molecular Simulations.

RESULTS AND DISCUSSION

Before designing a transducer, it is desirable that the properties of the active or passive piezoelectric material be fully characterized. In the case of P(VDF-TrFE), which is the material of choice for an application requiring thick slabs or unusually shaped designs, one needs first to select a suitable ratio of VDF and TrFE that crystallizes directly into the desired β-phase and that satisfies performance specifications of the transducer application. Thus, one of our primary objectives was to determine the effect of fluorine content on the relative stabilities of the α- and β-phases of PVDF and P(VDF-TrFE). We will discuss in the following sections how molecular modeling was used to study (1) the effect of polymer composition of the crystallization behavior of PVDF and P(VDF-TrFE) and (2) the determination of the electrical and mechanical properties of these materials.

THE CRYSTALLIZATION BEHAVIOR OF PVDF AND P(VDF-TrFE)

The crystal structures favored during crystallization of polymer melts or solutions are determined by the combined intermolecular and intramolecular energies. The intermolecular energies refer to the van der Waals and Coulombic interactions between neighboring chains packed in the unit cells. The intramolecular energies are determined by the chain conformation, i.e., the number and position of the *trans* and *gauche* linkages. The procedure used to study the energetics of crystallization is outlined in figure 9.

The initial structures used to build up larger chain segments were dimeric segments. The atomic positions of the dimers were determined by Hasegawa *et al.*, who employed x-ray crystallography.[34] These workers proposed that the PVDF α-phase is a distorted *tgtg'* structure, with a carbon dihedral repeating pattern of 179° and 45°.[34] According to the Hasegawa study, the β-phase conformation is a slightly distorted all-*trans* alternating planar zig-zag with repeating 172° and -172° angles.

P(VDF-TrFE) polymer segments were constructed from the PVDF segment by replacing the appropriate number of hydrogen atoms with fluorine atoms. The bond lengths and bond angles of the Hasegawa α- and β-phase structures are shown in table 5. Dimeric structures of PVDF and P(VDF-TrFE) were first minimized using semiempirical quantum mechanics. Atomic charges were calculated and assigned to each atom (figure 10). These segments were linked to together to form chains consisting of sixteen end-capped carbon atom structures. An extended structure of a PVDF chain is depicted in figure 11. Only one chain of PVDF was considered, since only one stereoregular arrangement of this polymer is possible. Although the structure of the carbon backbone of P(VDF-TrFE) is similar to that shown in figure 11 (with the exception that some hydrogen atoms are replaced by fluorine atoms), several arrangements of P(VDF-TrFE) are possible, however, since the monomers of these polymers can adopt *isotactic, syndiotactic,* and *atactic* configurations (figure 12). By configuration, we refer to the arrangement of fluorine and hydrogen atoms on each carbon center. In an isotactic polymer, all of the monomers have the same configuration. In an syndiotactic polymer, the configuration alternates from one monomer to the next. Atactic structures are random. In this study, only isotactic and syndiotactic structures were considered. Twelve structures of 75 mol% P(VDF-TrFE), where two TrFE monomers are separated by three VDF monomer units, were selected. The configurations of the two -CFH- centers represent isotactic and syndiotactic structures. Each structure of the 50 mol% P(VDF-TrFE) composition was also selected to represent isotactic and syndiotactic configurations. The sequences of all polymer chains consisted of head-to-tail linkages. No head-to-head or tail-to-tail sequences were considered.

The bond lengths, bond angles, and dihedral angles of the single carbon end-capped chains were optimized using molecular mechanics. The minimizations were

performed by allowing all of the atoms in the chain to relax. The resulting conformations were helical structures. The energies of these structures, which are tabulated in table 6, increase with fluorine content. The Hasegawa and "ideal" structures were then minimized *via* relaxation of the hydrogen and fluorine atoms while the positions of the carbon atoms in the polymer backbone chain were fixed. This approach allowed us to preserve the original geometry of the experimental chain conformation. When we compare the energies of each structure, we note that the Hasegawa *tgtg'* structure is more stable than the Hasegawa and "ideal" all-*trans* conformations. But the "ideal" all-*trans* structure is favored for the copolymers. A plot of the data (figure 13) shows that the crossover point, i.e., the composition where the "ideal" all-*trans* becomes more stable than the *tgtg'* is about 90 mol% VDF. These calculations agree with the well-documented experimental observation that PVDF is favored to crystallize into the *tgtg'* conformation, whereas the copolymer crystallizes into the all-*trans* structure.[35] The plots in figure 13 underscore the small differences in energy between the conformations. During annealing, however, formation of the most stable conformations will be favored.

To build crystal unit cells of PVDF and P(VDF-TrFE), chain segments were packed into a crystal unit cell. The direction of the polymer chain was aligned along the c-axis, and the structure was subsequently centered. There were no symmetry restrictions imposed on each unit cell. Starting with the initial structures based on x-ray data, the dimensions of the unit cells were minimized iteratively by calculating the energies of minor deformations in the lattice structures as well as rotations of the polymer chains about the c-axis (figure 14). The relaxed cell parameters of the PVDF and P(VDF-TrFE) unit cells are summarized in table 7. In agreement with x-ray studies, the a and b crystal dimensions increase with increasing fluorine substitution. This expansion of the cell lattice dimensions can be attributed to the increasing van der Waals energies as more fluorine atoms are added to the crystal structure. Examining the crystal energies (table 8), we note that the Hasegawa *tgtg'* crystal structure is favored over the "ideal" structure for all compositions. This calculation supports the Hasegawa structure,[36] and suggests that during crystallization from the melt or solution, the *t* and *g* dihedral bonds suffer distortions as the chains within the crystal lattice rotate. The energy required to distort the dihedral angles is probably more than offset by the energy gained during crystal packing.

The intramolecular energies calculated on the end-capped polymer chain segments and the resulting crystal packing energies are not additive in this study since these models do not have the same number of atoms. However, we can compare these energies and establish several important trends. The crystal packing energies of PVDF and P(VDF-TrFE) favor the all-*trans* conformation. For the copolymers, this is in line with the propensity of these compositions to crystallize into the all-*trans* β-phase. But the crystal packing calculations contradict the crystallization behavior of PVDF, which is known to crystallize directly into the *tgtg'* α- phase. One explanation for this discrepancy is that the intramolecular interactions play a

vital role in controlling the kinetics of crystallization. During crystallization, although the energy of the all-*trans* PVDF unit cell is lower than the energy of the *tgtg'* cell, a large energy barrier may prevent crystallization into the β-phase. This barrier is somewhat relaxed for the copolymer compositions so that crystallization into the β-phase is favored both kinetically and thermodynamically. Recent calculations using molecular dynamics have been undertaken in this laboratory and support this idea. These results will be reported in the near future.[37]

The most important conclusion of this portion of the study is that these calculations demonstrate that crystallization into the desired β-phase is favored for P(VDF-TrFE) compositions where VDF is less than 90 mol%. This knowledge allowed us to set an upper limit on the percent composition of VDF to achieve the β-phase without mechanical stretching. Ideally, the VDF concentration should be as high as possible to also maximize the Curie temperature, which is the crystal-crystal transition between the lower temperature ferroelectric phase and the higher temperature paraelectric phase. Above the Curie temperature, the polymer looses its polarization. Since the Curie temperature increases from about 125°C at VDF ≈ 60 mol% to over 180°C for PVDF,[5,38,39] to satisfy the contradictory requirements of energetics and temperature stability, the most suitable copolymer compositions should be those with VDF content between 60 and 90 mol%.

CALCULATION OF THE ELASTIC MODULI AND PIEZOELECTRIC CONSTANTS

When a piezoelectric polymer unit cell is stressed, the resulting strains along the c-axis (the chain direction), a-axis, and b-axis (poling direction) can be written as

$$S_c = s_{11}^c T_1 + s_{12}^c T_2 + s_{13}^c T_3, \tag{29}$$

$$S_a = s_{21}^c T_1 + s_{22}^c T_2 + s_{23}^c T_3, \tag{30}$$

and

$$S_b = s_{31}^c T_1 + s_{32}^c T_2 + s_{33}^c T_3, \tag{31}$$

where S_c, S_a, and S_b are, respectively, the strains along the c, a, and b directions, s_{ij}^c is the real elastic compliance (i,j = 1, 2, and 3), and T_1, T_2, and T_3 are the applied stresses in the c, a, and b directions, respectively (figure 15). When a stress, T_3, is

applied to an unclamped crystal cell along the direction of the poling field, then

$$(s_{33}^{c}+s_{23}^{c}+s_{13}^{c})T_3=s_{33}^{c'}T_3, \tag{32}$$

where $s_{33}^{c'}$ is the compliance of an unclamped crystal cell. We will assume for now that the c-axis is clamped, that is when the b-axis is stretched, the a-axis deforms but the c-axis does not change its dimension. Thus, from equation (29), the stress of a crystal clamped in the chain or c-axis direction ($S_c = 0$; $T_2 = 0$) can be written as

$$T_1=-\frac{s_{31}^{c}}{s_{11}^{c}}T_3. \tag{33}$$

Note that we have assumed that $s_{13}^{c} = s_{31}^{c}$. So if the c-axis is clamped and $S_c = 0$, then

$$S_b+S_a=(s_{21}^{c}+s_{31}^{c})T_1+(s_{23}^{c}+s_{33}^{c})T_3. \tag{34}$$

With the further assumption that $s_{31}^{c} \approx s_{21}^{c}$, we obtain from equations (33) and (34)

$$[s_{33}^{c}+s_{23}^{c}-\frac{2(s_{31}^{c})^2}{s_{11}^{c}}]T_3=s_{33}^{c''}T_3. \tag{35}$$

The effective compliance of the clamped cell, $s_{33}^{c''}$, is therefore

$$s_{33}^{c''}=s_{33}^{c'}-s_{13}^{c}[1+\frac{2s_{13}^{c}}{s_{11}^{c}}]. \tag{36}$$

The procedure to calculate the elastic compliances is based on a curve-fitting method to calculate the tensile compliance of long-chain polymers with molecular

modeling techniques.[40] As adapted to the present work, the procedure consisted of the application of tiny homogeneous stresses to the plane of the polymer unit cell normal to the poling or "3" direction. In the case of a PVDF crystal, since the unit cell is orthorhombic, only the a-dimension was permitted to undergo relaxation. The c-dimension was clamped. The intermolecular energy consisting of van der Waals and electrostatic interactions was calculated for each deformed structure. The energies and deformations were then subjected to curve-fitting by linear regression to the cubic form of

$$E_{vdW+e}=A(\Delta b)^3+\frac{K}{2}(\Delta b)^2+B(\Delta b)+C, \tag{37}$$

where K is the force constant of the deformation Δb, E_{vdW+e} is the sum of the vdW and electrostatic energies, and A, B, and C are constants. The force constant, K, was calculated from the slopes of equation (37). The correlation coefficient of each curve was at least 0.9998. As exemplified by a plot of K *vs.* elongation of a PVDF unit cell (figure 16), the force constant typically displayed wide excursions at deformations less than 0.05%. Accordingly, the force constants were determined within the ranges of deformations represented by the flat regions of the curves. Thus, the elastic compliance associated with changes in the b-dimension of the crystal unit cell, $s_{33}^{c''}$, is

$$s_{33}^{c''}=\frac{1}{K}\frac{ac}{b}, \tag{38}$$

where ac is the area of the plane perpendicular to the direction of the deformation.

The elastic compliance, s_{11}^{c}, was calculated by simulating a stretching of a single polymer chain along the c-axis.[41] A semiempirical quantum mechanical approach was chosen for chain minimization since a previous semiempirical study demonstrated good agreement between calculated and experiment tensile moduli of several polymer chains.[40,42] In this case, the heat of formation of each structure was calculated. Each of these chain structures was then packed into a crystal cell whose a- and b-dimensions were subsequently minimized. The minimized energies and b-dimensions were then used to calculate s_{13}^{c}.

The elastic compliances are tabulated in table 9. The values listed here show that the difference between $s_{33}^{c'}$ and $s_{33}^{c''}$ of a unit cell of PVDF and the 50 mol% copolymer is less than 1%, i. e., $s_{33}^{c'} \approx s_{33}^{c''}$. This can also be assumed to be the case for the 75 mol% P(VDF-TrFE).

We now turn to the calculation of changes in polarization when a crystal cell is

deformed. Stressing a polymer unit cell in the direction of the poling field induces a change in its volume and saturation polarization:[33]

$$d_{33}^{c}=\frac{P_s^f-P_s^i}{T_3}, \tag{39}$$

where d_{33}^{c} is the piezoelectric constant, and P_s^i and P_s^f are the initial and final saturation polarizations. We define the saturation polarization of a polymer unit cell as[43,44,45]

$$P_s=\frac{\sum \mu_k}{v_c}, \tag{40}$$

where μ_k is the dipole moment of an individual C-F bond and v_c is the volume of the unit cell. The procedure to calculate the total dipole moments of PVDF and P(VDF-TrFE) crystal cells is based on the rigid dipole model.[46] In this approach, the dipole moments of the individual C-F within a packed unit cell were summed to obtain the total dipole moment of the cell. The changes in cell volume and polarization, and the piezoelectric constants were calculated by simulating stresses along the b-axis of the minimized crystal structures (table 9). The calculated s_{33}^{c} elastic compliance and d_{33}^{c} piezoelectric constants of the crystals are also tabulated in table 9. These data suggest that the crystals of PVDF and P(VDF-TrFE) are "hard" materials and that fluorine substitution decreases the compliance along the b-axis. A possible explanation for the low compliance may be found in the interactions taking place during deformation of the lattice dimensions. Changes in the lattice geometry of the cell are accompanied by unfavorable van der Waals interactions between fluorine atoms on adjacent chains.

The values here, which are smaller than those obtained by Goddard and Karasawa[47] and Tashiro *et al.*,[33] suggest that polymer crystals by themselves are low compliance materials and therefore possess low levels of piezoelectricity. However, the results of the calculations in this work are not inconsistent with the well-known piezoelectric properties of *semicrystalline* PVDF and P(VDF-TrFE), if, as will be demonstrated below, the origin of piezoelectricity in the semicrystalline polymers lies in the properties of both the crystalline and amorphous phases. In this model,

the Young's modulus of a semicrystalline polymer can be written as[33]

$$Y_{33}^{sc} \approx Y_{33}^{a}(1-X_c)+X_c Y_{33}^{c}, \tag{41}$$

where Y_{33}^{sc} and Y_{33}^{a} are the Young's moduli of the semicrystalline polymer and amorphous phase, respectively, and X_c is the degree of crystallinity. The Young's modulus of a semicrystalline polymer of known crystallinity, Y_{33}^{sc}, can be obtained from the literature. On substitution of the literature value into equation (41), s_{33}^{a} can be calculated ($Y_{33} = 1/s_{33}$). It is likely that s_{33}^{a} is independent of crystallinity, so that equation (41) can also be used to estimate s_{33}^{sc} of piezoelectric polymers possessing varying crystallinities.

The piezoelectric constant of a semicrystalline polymer is calculated from[48]

$$d_{33}^{d} = -s_{33}^{sc}\theta X_c P_s, \tag{42}$$

where d_{33}^{d} is the piezoelectric response due to dimensional changes, and θ is the average orientation of dipoles along the poling direction.

We have calculated the s_{33} elastic compliances and d_{33} constants for hypothetical semicrystalline PVDF and 75 mol% P(VDF-TrFE) compositions using equations (41) and (42). These are the *predicted* values for semicrystalline polymers. Consider first the calculation for PVDF. An experimental compliance of PVDF with $X_c = 0.5$ was taken to be 4.72×10^{-10} m^2/N.[49] Elastic compliance values were calculated for PVDF possessing different degrees of crystallinity. From the elastic compliance and polarization, we calculated the piezoelectric constant. As shown in table 10, the experimental d_{33} values agree well with the calculated d_{33}^{d} values for those compositions where $X_c = 0.5$. For 75 mol% P(VDF-TrFE), s_{33}^{a} was calculated using the experimental elastic compliance, 3.0×10^{-10} m^2/N for $X_c = 0.75$.[16] We took into account the possibility of local-field effects for 75 mol% P(VDF-TrFE). It is known that local-field effects may enhance the saturation polarization of the 75 mol% P(VDF-TrFE) unit cell.[43] Including this local-field correction improves the agreement between the experimental and calculated d_{33}^{d} constants for the 75 mol% P(VDF-TrFE) copolymer (local-field corrections for PVDF can be neglected[50,51]). Again, as in the case of PVDF, the agreement between the experimental and calculated piezelectric constant is good.

There are several conclusions to be drawn from this treatment. First, the maximum d_{33}^{d} occurs at compositions that are about 50% crystalline, and d_{33}^{d} is predicted to decrease at higher crystallinities. This is not surprising in light of our calculation that predicts "hard" crystallites. Another conclusion is that a significant decrease in piezoelectricity should occur at low crystallinites due to low crystal

polarizations. Both of these conclusions allow us to portray the microstructure of semicrystalline polymers as a collection of oriented C-F dipoles embedded in a "soft" amorphous phase.[52] The piezoelectric response is therefore a result of small motions of these dipoles. The key feature of this model is that the polymer can be treated as a composite of tiny but polarized crystallites immersed in a nonpolarized, relatively soft amorphous polymer.

CONCLUSIONS AND RECOMMENDATIONS

The original objective of this work was to demonstrate that molecular modeling is a practical methodology to aid in the proper selection, preparation, and processing of piezoelectric fluoropolymers for transducer applications. The impetus for such an undertaking was to broaden our practical knowledge of these complex materials. It was hoped that by modeling the atomic and molecular properties of PVDF and P(VDF-TrFE) in an effort to identify the most suitable compositions for hydrophone and projector applications that sufficient "in-house" knowledge would be acquired to maximize the practical application of these materials. Such an effort would naturally lead to a procedure where one would select the composition and subsequent processing conditions from a knowledge of the final transducer properties and performance. This procedure might be called "molecular tailoring" or design of transducer materials, and could be conceived as an algorithm where the transducer designer might enter the desired parameters of a transducer application such as a figure of merit (FOM) and obtain the materials properties such as degree of crystallinity, polarization, and elastic complicance that would result in the desired FOM. That we are at the threshold of such a procedure is evidenced by our success in confirming certain well-known properties of PVDF and the copolymers through computational chemistry techniques and by the success we have had in building a multilayered copolymer stack for an active projector.[5] In the meantime, this project has lead to several interesting and practical conclusions concerning PVDF and P(VDF-TrFE).

1. We have identified P(VDF-TrFE) compositions that should be suitable for most piezoelectric applications requiring unusual shapes or thick slabs of copolymer. These may be applications where mechanical stretching (as in the case of PVDF) would be difficult to perform. The calculations in this work, which were carried out on copolymer model molecules, suggest that compositions containing between 60 and 90 mol% VDF crystallize directly into the β-phase, have sufficient polarization, and possess Curie transitions sufficiently high to rule out the possibility of depoling during long periods of use under moderate temperature conditions. It is recommended that attention be given to those copolymers having these levels of VDF.

2. The results of the elastic compliance study, although still tentative, suggest that piezoelectric crystals are by themselves low compliant materials and that piezoelec-

tricity arises from the collective motion of dipoles embedded in the soft amorphous phase of the polymer. If this is true, then the optimum crystallinity would be at about $X_c = 0.5$. This degree of crystallinity can be achieved by carefully monitoring the annealing conditions and by performing differential scanning calorimetry. At this stage, it is recommended that more attention be given to the effects of crystallinity on piezoelectric performance and also on long term aging. It is also suggested that further investigation be given to checking and testing the hypothesis suggested by the results of this study that piezoelectric fluoropolymeric crystals are indeed "hard."

3. A final recommendation is suggested by the focus, in this study, on the molecular properties of fluoropolymers. Although attention was given to PVDF and P(VDF-TrFE), there are other molecular combinations to consider. With only a few exceptions, little work has been done on other fluoropolymeric systems, including, for example, copolymers of vinyl fluoride and vinylidene fluoride, tetrafluoroethylene and vinylidene fluoride, to name only a few. It would be a fruitful enterprise to study the intramolecular and crystal packing energies of these copolymers as well as their polarizations and elastic compliances, using the techniques described in this report, and to compare these values with the data for PVDF and P(VDF-TrFE). Such an enterprise might reveal superior performance properties and lead to the development of new and exotic transducer materials.

In conclusion, this project demonstrates the validity and practicality of using a "molecular" approach for the study of material properties. As molecular modeling matures, computational chemistry will emerge as a powerful tool to sort out the complexities of candidate materials for practical applications such as described in this report.

HOMOPOLYMER: - A - A - A - A - A - A -

COPOLYMER: - A - B - A - B - A - B - (ALTERNATING)

- A - A - B - A - B - B - A - B - (RANDOM)

A , B = MONOMERS

Figure 1. Representation of the Chain Structures of Polymers

PVDF:

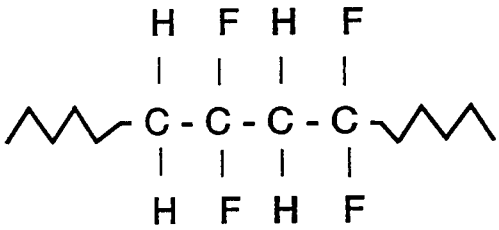

P(VDF -TrFE):

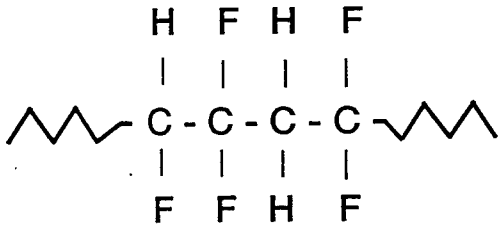

Figure 2. Extended Molecular Structures of PVDF and P(VDF-TrFE) Chain Segments

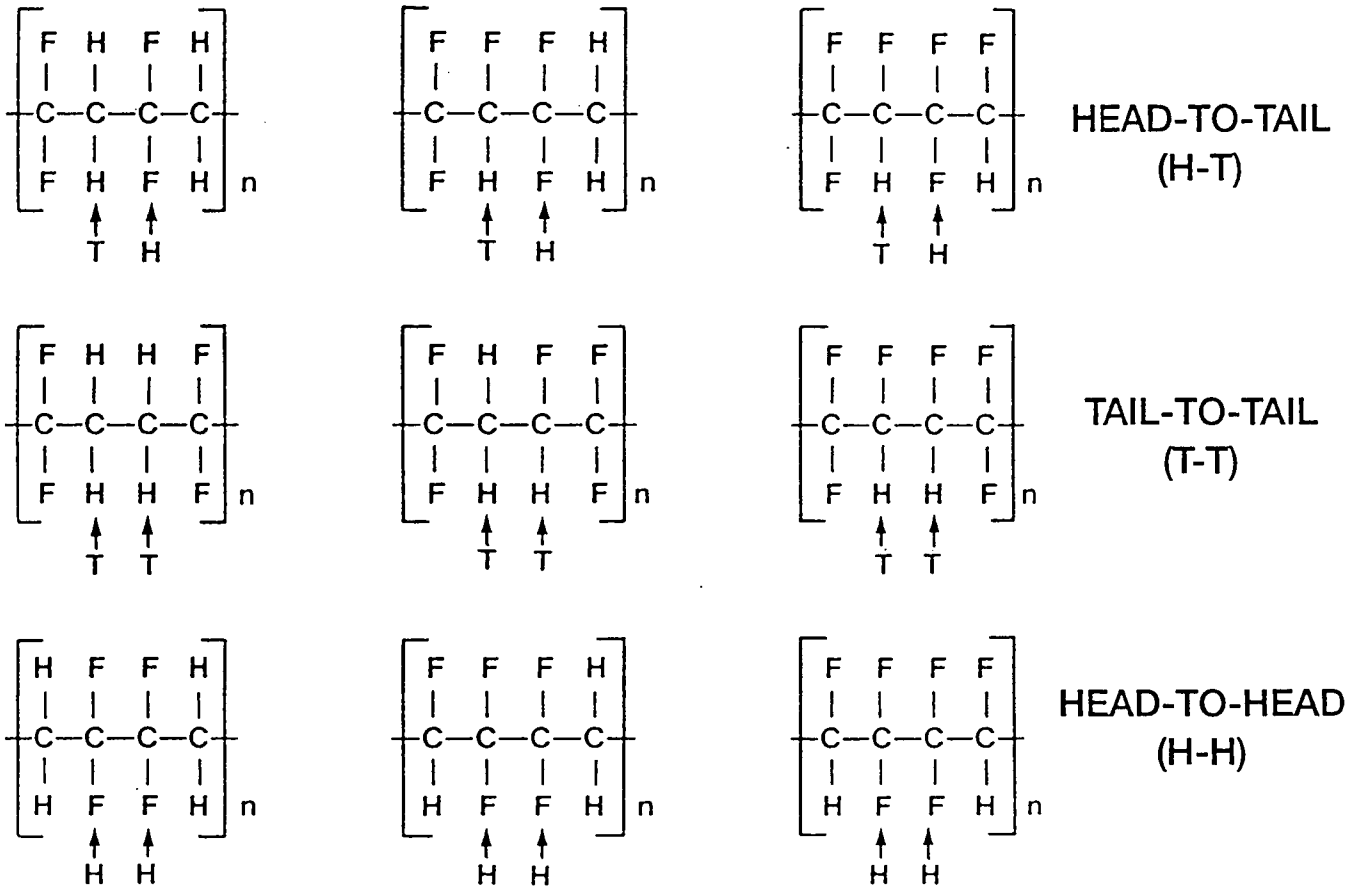

Figure 3. Extended Molecular Structures Showing Chain Connectivity

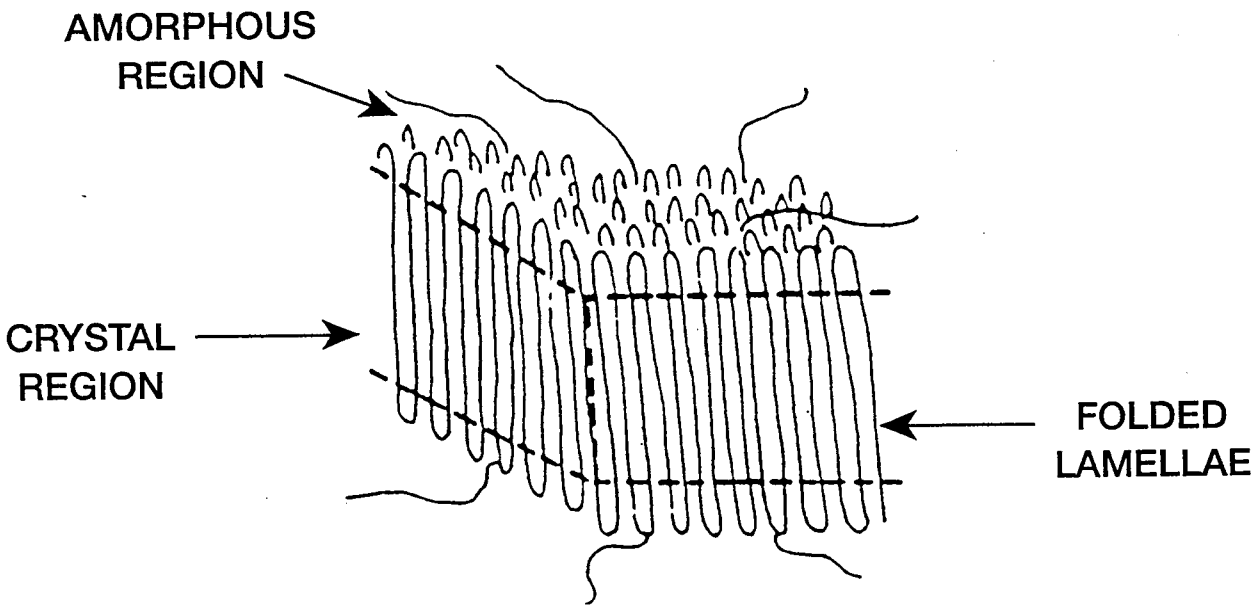

FROM: STEVENS, "POLYMER CHEMISTRY: AN INTRODUCTION",
2ND ED., OXFORD UNIVERSITY PRESS: OXFORD, 1990, P.92

Figure 4. Stacks of Lamellar Polymers

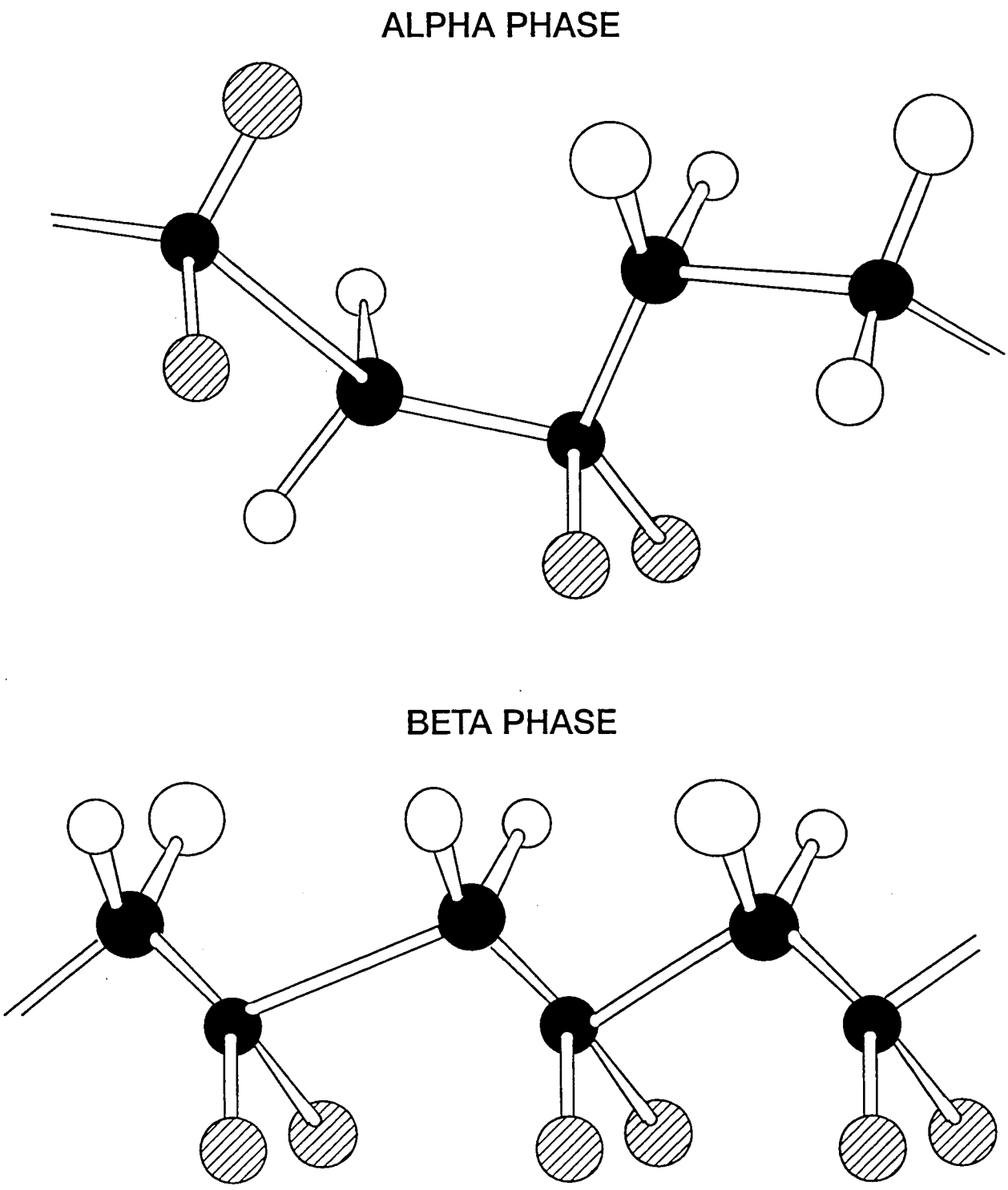

Figure 5. Chain Conformations of the α- and β-Phases

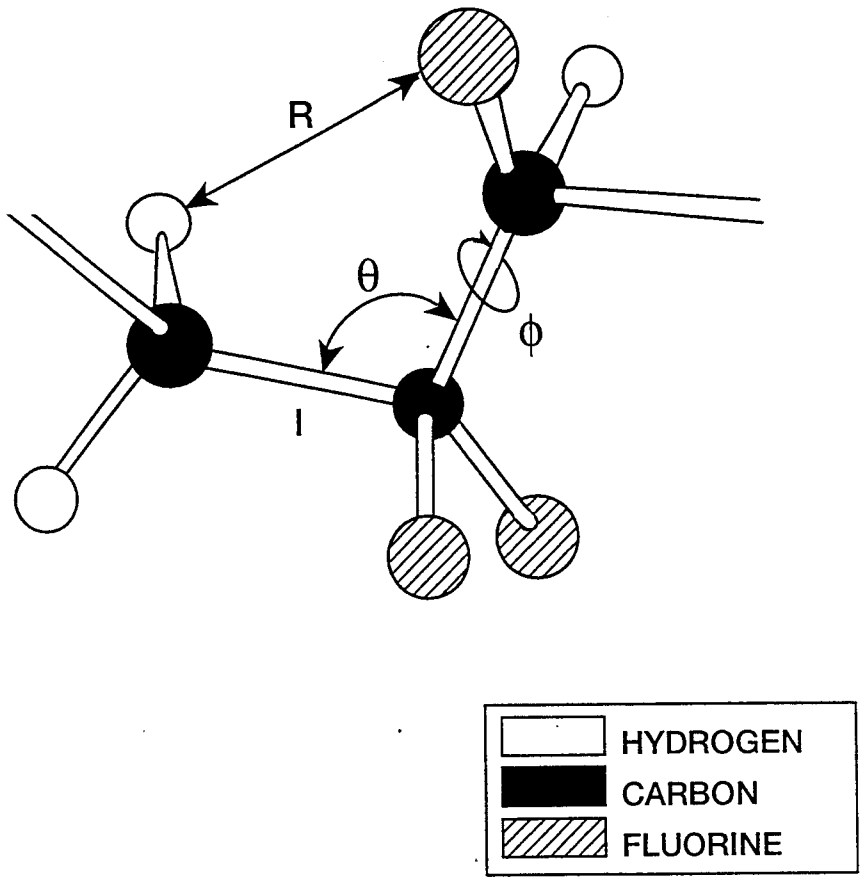

Figure 6. Bond Lengths, Bond Angles, Dihedral Angles, and Nonbonded Distances

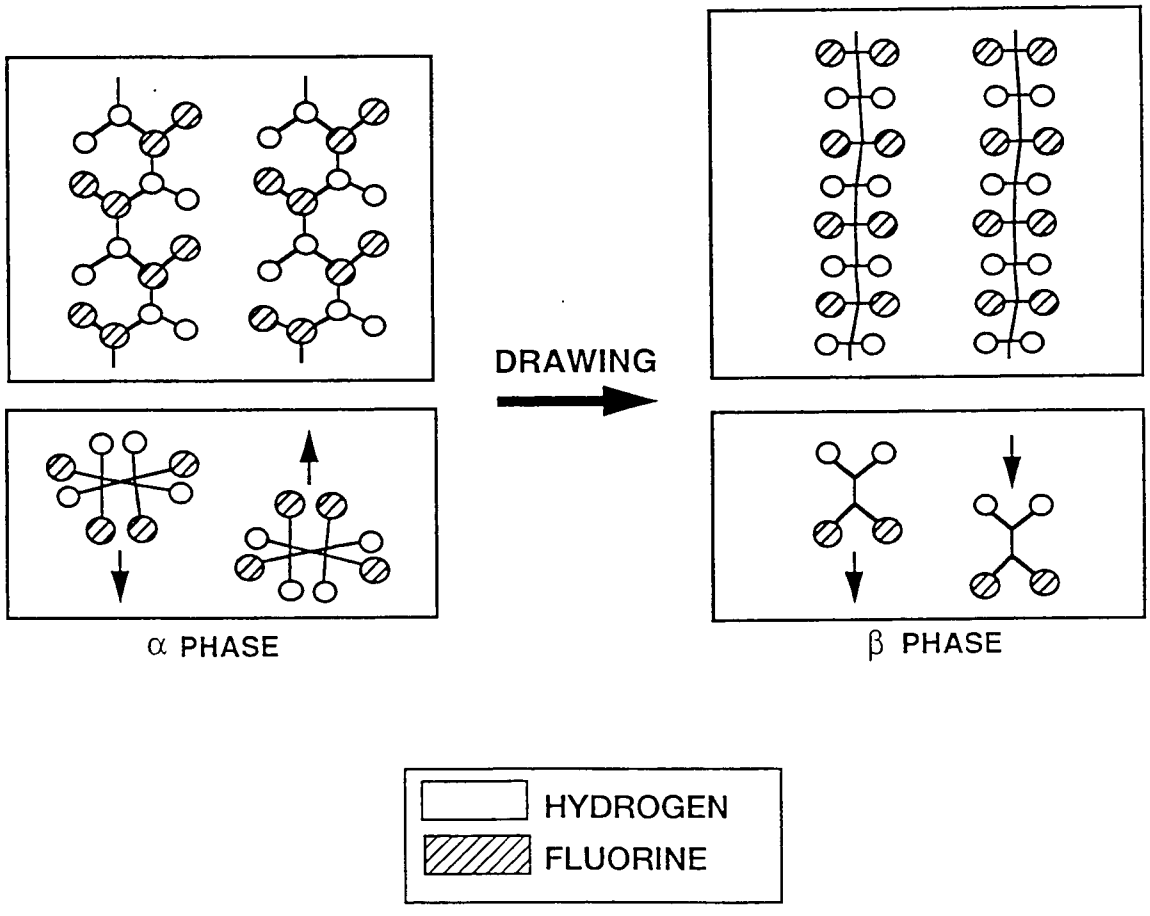

Figure 7. Crystal Structures of the α- and β-Phases

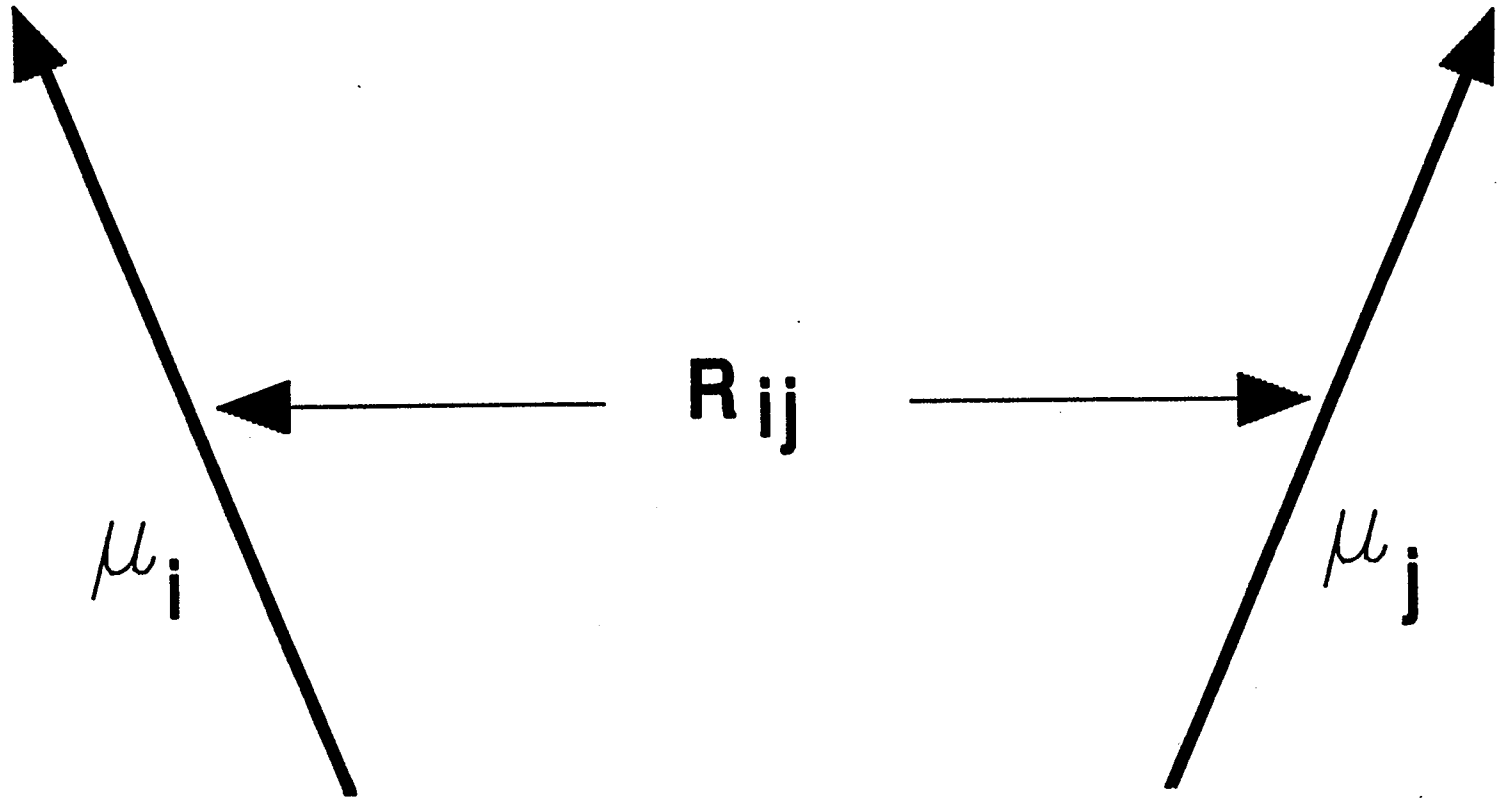

Figure 8. Dipole-Dipole Interactions

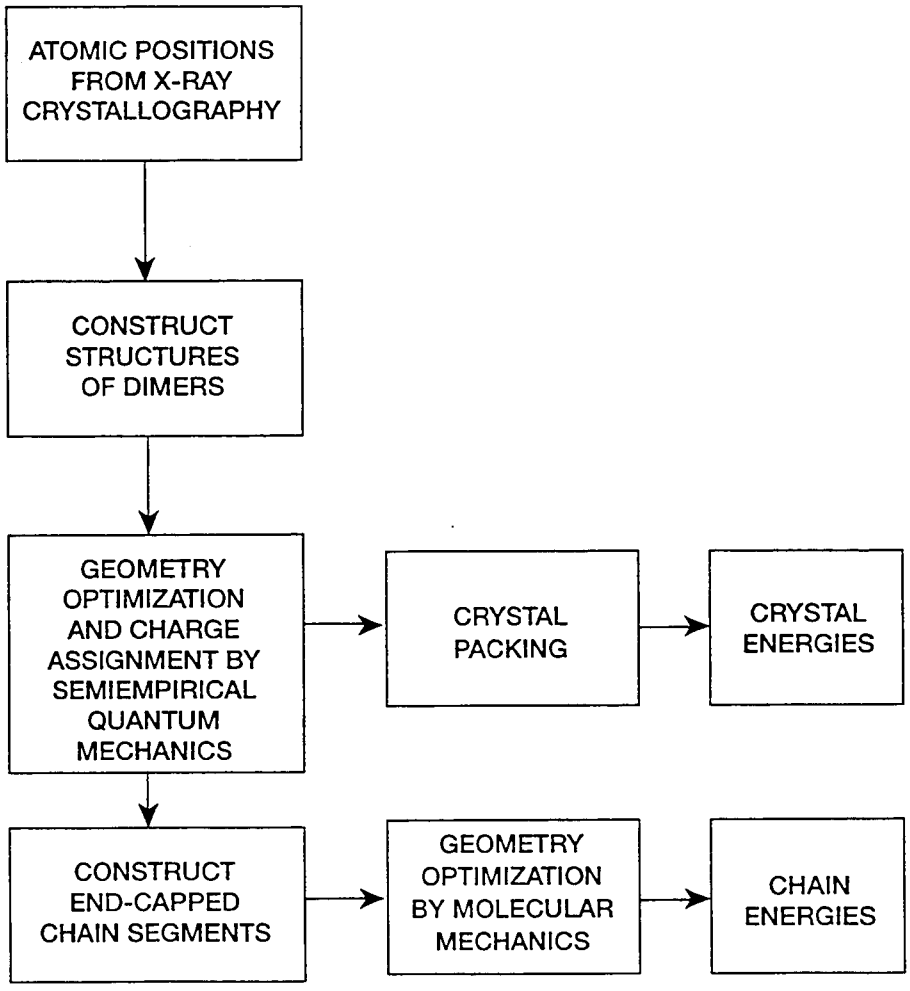

Figure 9. Flow Chart Used to Study the Energies of Crystals and Chains

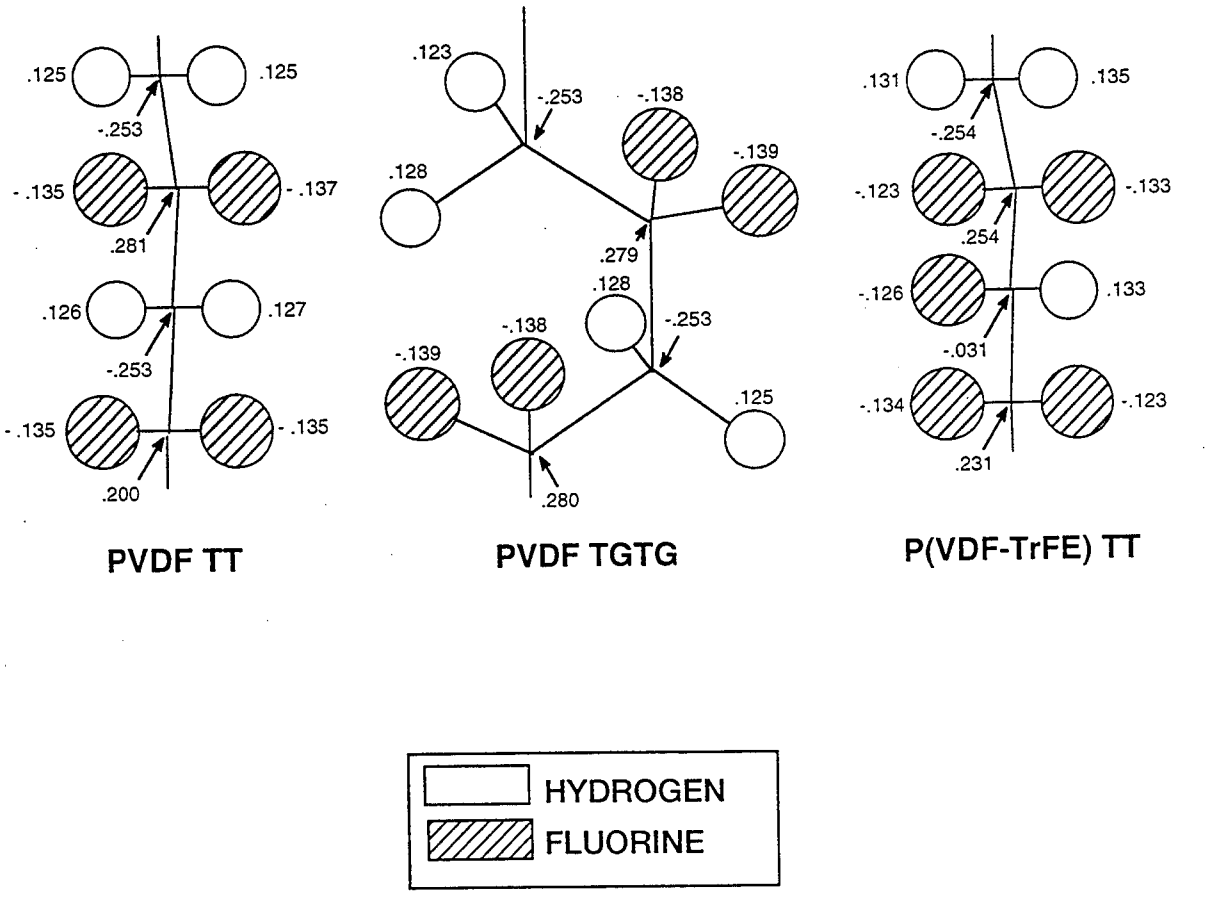

Figure 10. Atomic Charges Calculated by Semiempirical Quantum Mechanics

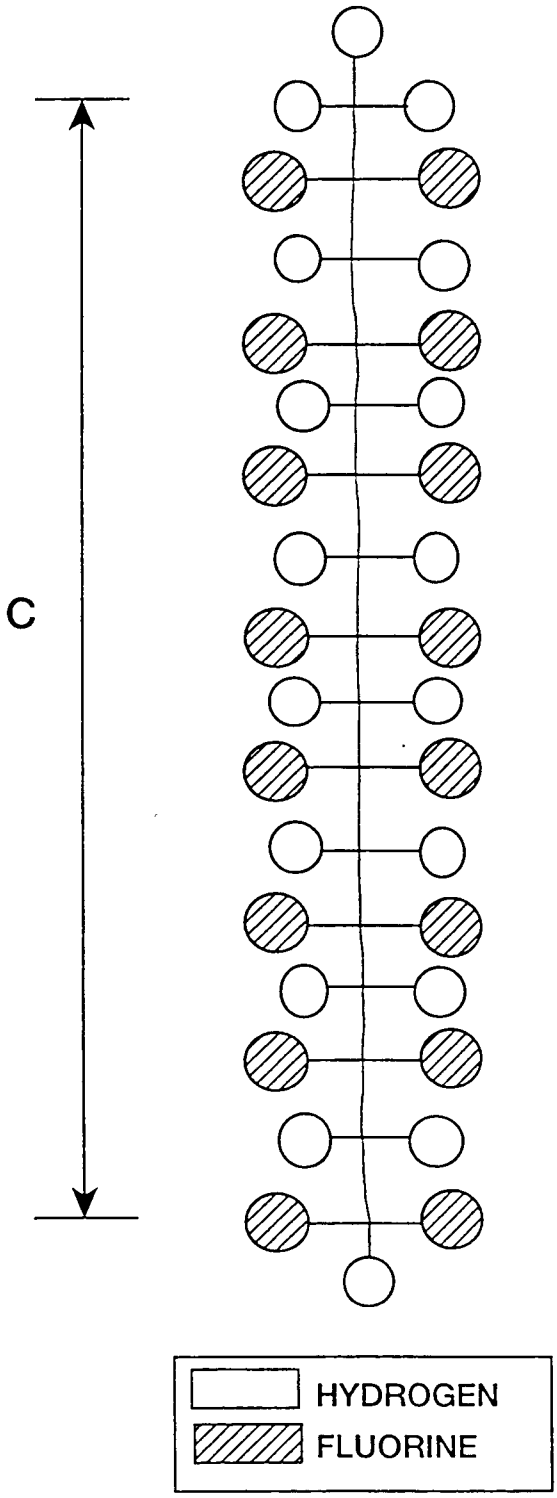

Figure 11. Extended Structure of PVDF End-Capped Polymer Chain

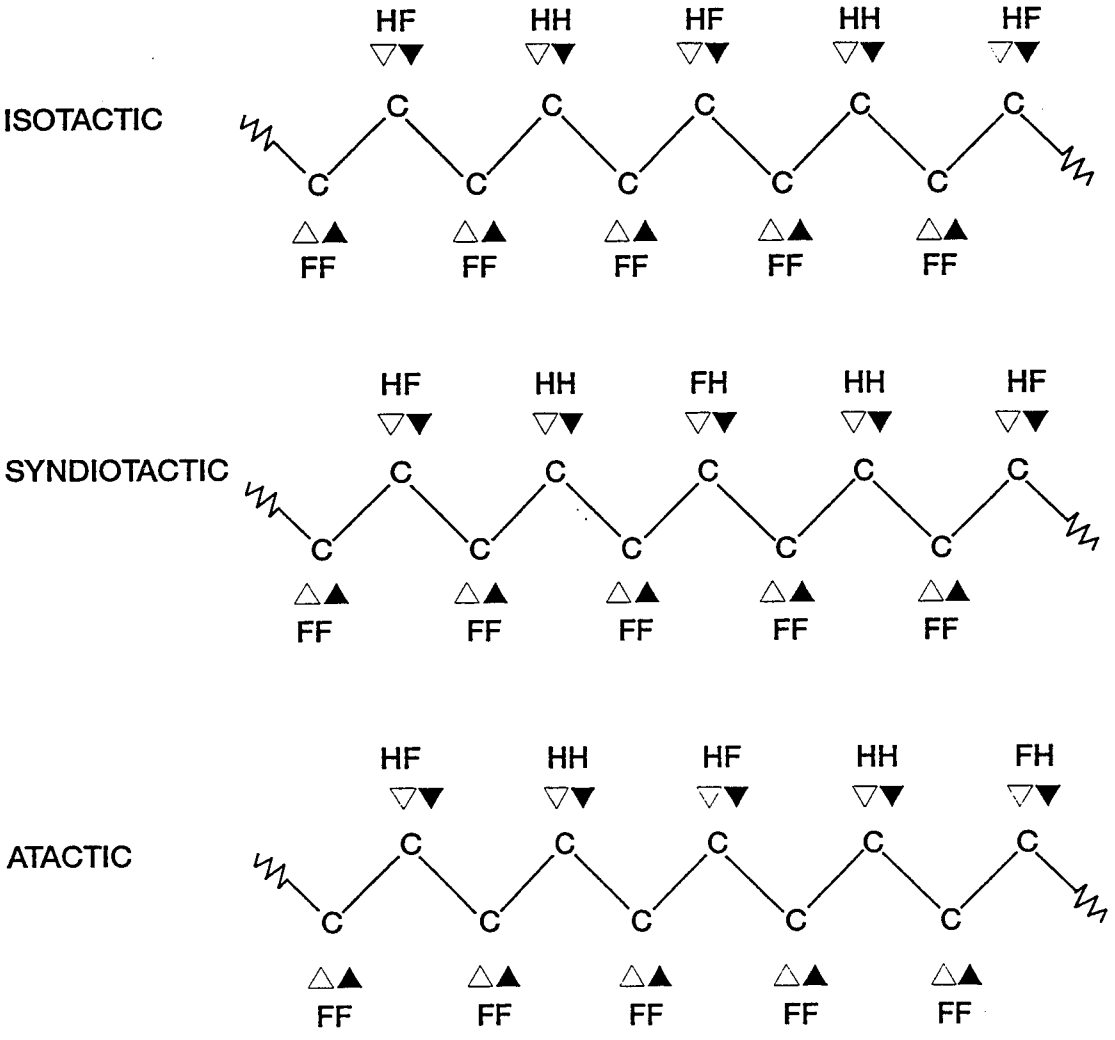

Figure 12. Isotactic, Syndiotactic, and Tactic Structures

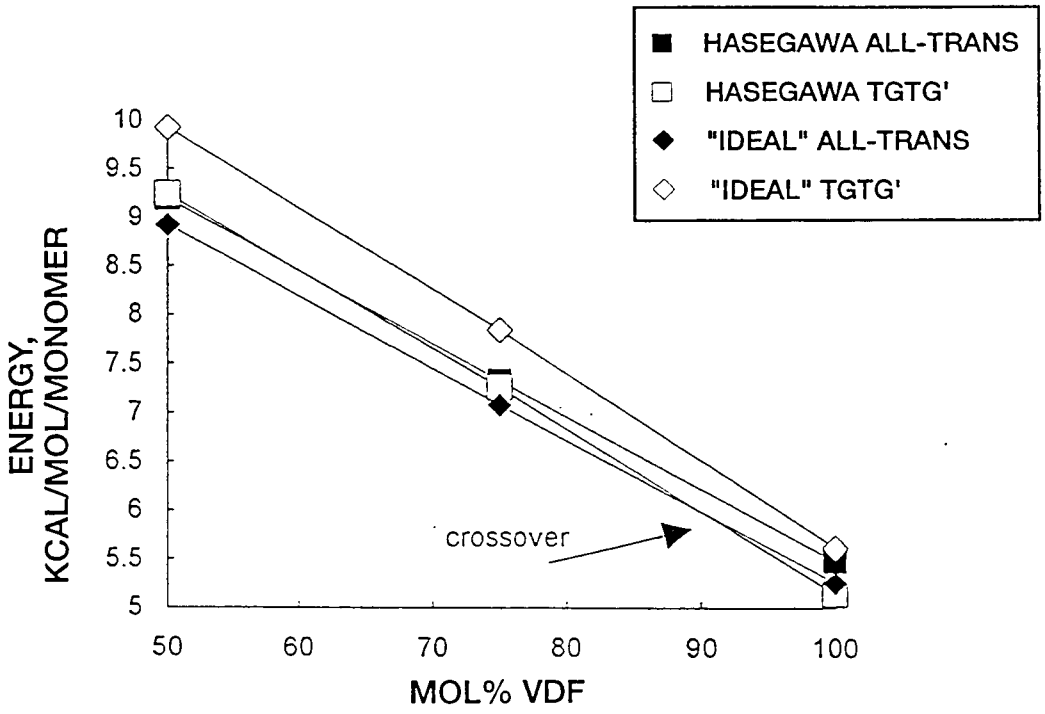

Figure 13. Conformational Energies of P(VDF-TrFE) Compositions

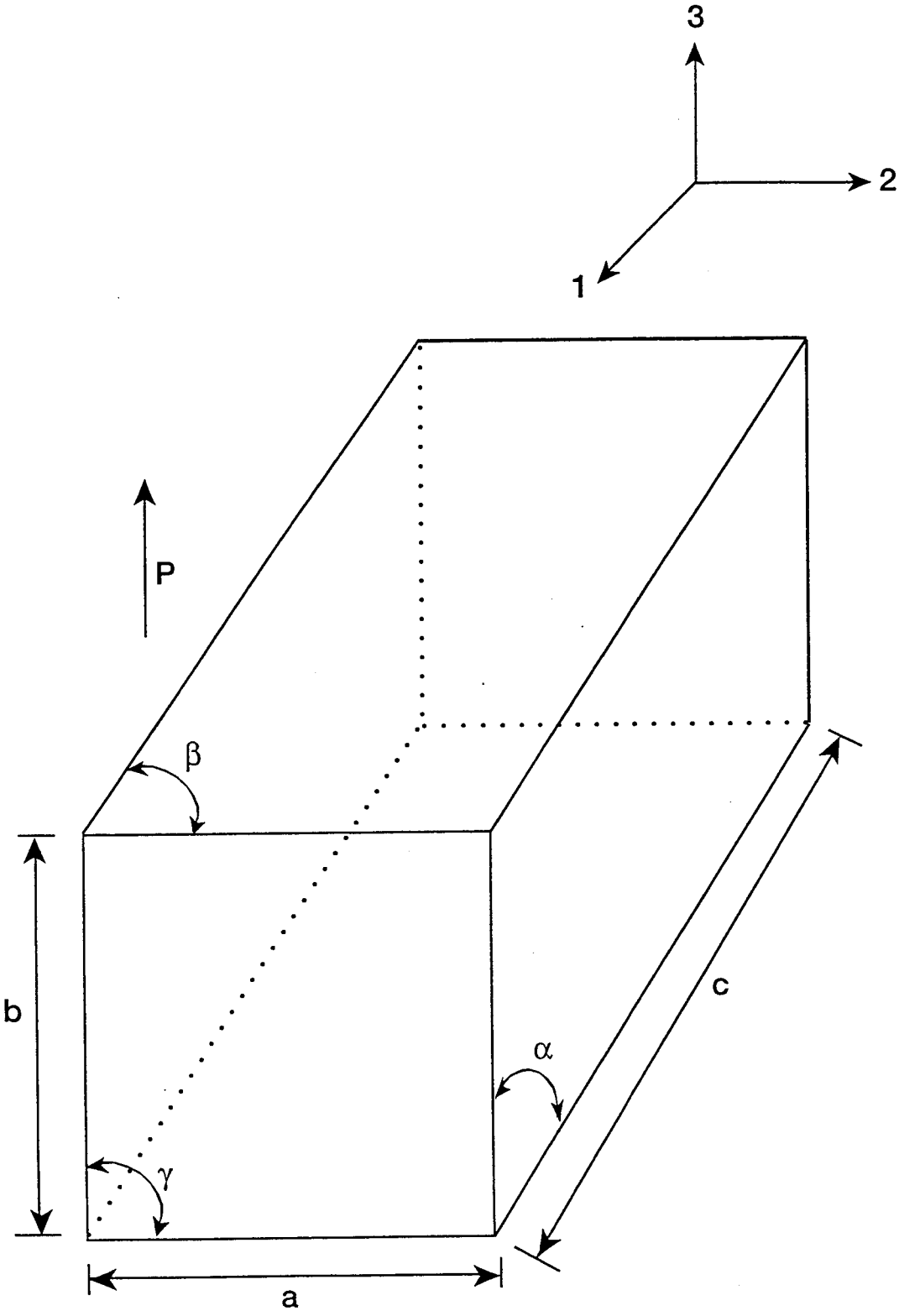

Figure 14. Polymer Unit Cell

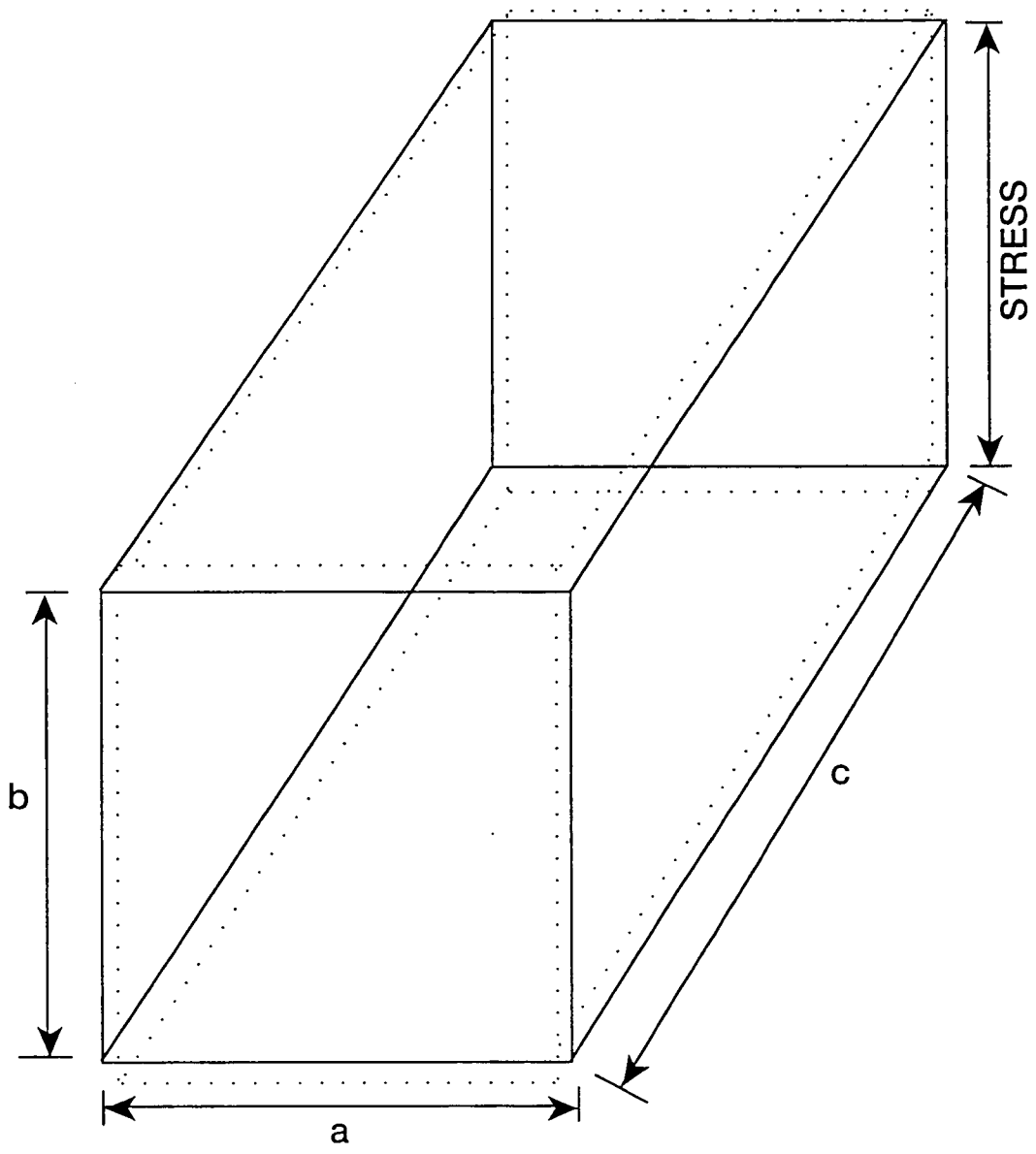

Figure 15. Crystal Undergoing Stress

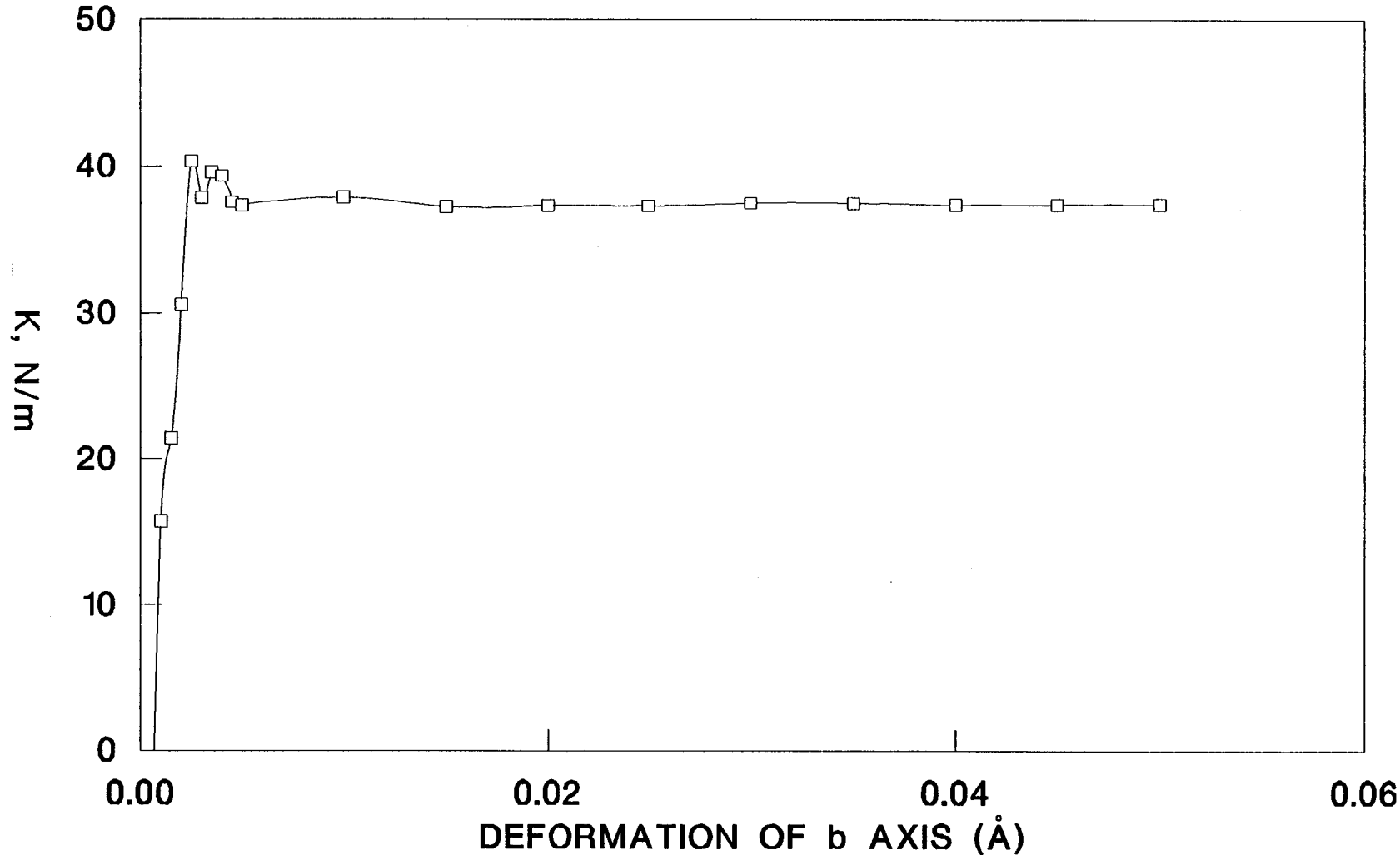

Figure 16. Force Constant Versus Elongation of b-Dimension

Table 1. Molecular Mechanics Bond-Length Parameters[a]

Bond	l_o Å	k_s mdyn /Å
C-C	1.523	4.400
C-H	1.113	4.600
C-F	1.392	6.100

[a]Reference 27.

Table 2. Molecular Mechanics Bond-Angle Parameters[a]

Bond Angle	θ_o Å	k_b mdyn Å/rad
C-C-C	109.5	0.450
C-C-H	109.4	0.360
H-C-H	109.5	0.320
F-C-F	107.1	1.070
F-C-H	110.5	0.490
C-C-F	109.0	0.650

[a]Reference 27.

Table 3. Molecular Mechanics Dihedral Parameters[a]

Bond Angle	V_1 kcal/mol	V_2 kcal/mol	V_3 kcal/mol
C-C-C-C	0.2000	0.270	0.093
C-C-C-H	0.000	0.000	0.267
C-C-C-F	0.000	-0.086	0.930
H-C-C-H	0.000	0.000	0.237
H-C-C-F	0.000	0.000	0.351
F-C-C-F	-0.1000	-2.000	0.200

[a]References 22 and 27.

Table 4. Molecular Mechanics Nonbonded Parameters[a]

Atom	r Å	ε kcal/mol
C	1.9000	0.0440
H	1.5000	0.0470
F	1.6500	0.0780

[a]References 22 and 27.

Table 5. Molecular Parameters of Hasegawa Structures[a]

Parameter		α-Phase	β-Phase
l	C-C C-F C-H	1.54 Å 1.34 Å 1.09 Å	1.54 Å 1.34 Å 1.09 Å
θ	C-C-C	118.5°, 116.5°	112.5°
ϕ	C-C-C-C	179°, 45°	171.6°

[a]Reference 35.

Table 6. Energies of End-Capped Helical Chains[a]

mol% VDF	Polymorph	Hasegawa	"Ideal"	Minimized
100%	all-*trans*	5.48	5.26	4.86
	tgtg'	5.14	5.63	5.09
75%	all-*trans*	7.33	7.08	6.58
	tgtg'	7.26	7.85	7.05
50%	all-*trans*	9.19	8.92	8.37
	tgtg'	9.24	9.92	8.87

[a]Steric energies are in kcal/mol/monomer.

Table 7. Calculated and Experimental Lattice Dimensions and Angles of PVDF and P(VDF-TrFE)[a]

mol% VDF	Lattice dimensions, Å			Lattice angles, deg			Crystal system
	a	b	c	α	β	γ	
100	8.99 (8.58[b])	4.88 (4.91[b])	2.56 (2.56[b])	90 (90[b])	90 (90[b])	90 (90[b])	orthorhombic
75	9.08 (8.86[c])	5.11 (4.62[c], 5.12[d])	(2.56[c])	90.01 (90[c])	89.9 (90[c])	95.2 (90[c])	monoclinic
50	9.10 (9.12[e])	5.27 (5.25)	2.56 (2.55)	86.6 (93)	87.5	96.3	monoclinic

[a]Experimental values, where available, are shown in parenthesis.

[b]Reference 34.

[c]H. Ohigashi and K. Koga, " *Japanese Journal of Applied Physics*, vol. 21, 1982, p. L455.

[d]78 mol% P(VDF-TrFE); A. J. Lovinger, T. Furukawa, G. T. Davis, and M. G. Broadhurst, "Crystallographic Changes Characterizing the Curie Transition in Three Ferroelectric Copolymers of Vinylidene Fluoride and Trifluoroethylene: 1. As-crystallized Samples," *Polymer Papers*, vol. 24, 1983, p. 1225.

[e]55 mol% P(VDF-TrFE), low-temperature phase; Tashiro K., Takano, K., Kobayashi, M., Chatani, Y., and Tadokoro, H. *Ferroelectrics* 1984, 57, 297.

Table 8. Calculated Crystal Packing Energies[a]

		Hasegawa			Ideal		
mol% VDF	Polymorph	vdW	Coul.[b]	Total Energy	vdW	Coul.	Total Energy
100	all-*trans*[c]	-4.77	-2.41	-7.19	-5.04	-2.47	-7.51
	tgtg' [d]	-4.21	-0.11	-4.32	-3.82	0.36	-3.47
75	all-*trans*[e]	-4.73	-1.78	-6.44	-4.85	-1.75	-6.60
	all-*trans*[c]	-4.62	-1.72	-6.34	-4.83	-1.75	-6.58
	tgtg' [d]	-4.33	-0.47	-4.80	-3.92	-0.12	-4.04
50	all-*trans*[e]	-4.63	-1.07	-5.70	-4.85	-1.10	-5.96
	all-*trans*[c]	-4.59	-1.04	-5.64	-4.82	-1.14	-5.94
	tgtg' [d]	-4.28	0.88	-3.40	-3.67	0.89	-2.78

[a]Energies are in kcal/mol/monomer. Crystal packing simulations on α- and β-phase superlattice cells were performed with CERIUS Version 3.1 Software (Molecular Simulations) for the Silicon Graphics 4D/35 Personal Iris workstation.

[b]Coulombic interactions were calculated using the Ewald summation technique.

[c]The symmetry was assumed to be orthorhombic for planar zigzag ("ideal") and alternatively deflected (Hasegawa) structures. During crystal packing, the a and b unit cell dimensions and the setting angles were allowed to relax. Symmetry remains orthorhombic during crystal packing when α, β, and γ cell angles are allowed to relax.

[d]Structure of *tgtg'* unit cell was assumed to be monoclinic. Crystal packing energies were determined by relaxing a and b unit cell dimensions and the setting angles.

[e]Monoclinic symmetry. a and b dimensions, α, β, and γ cell angles, and the setting angles were allowed to relax.

Table 9. Calculated Elastic Compliances and d Constants of PVDF and P(VDF-TrFE) β Crystals

Polymer	s_{33}^{c}, m^2/N ($x10^{-11}$)	s_{11}^{c}, m^2/N ($x10^{-11}$)	s_{31}^{c}, m^2/N ($x10^{-11}$)	T_3, N/m^2 ($x10^8$)	ΔP_s mC/m^2	d_{33}^{c}, pC/N
PVDF	2.59 (8.06[a], 9.52[b])	0.2	-0.037	3.95	-0.00132	-3.3 (-18.8[a], -25[b])
75 mol% P(VDF-TrFE)	3.97	0.19	-	2.46	-0.00252	-4.0
50 mol% P(VDF-TrFE)	5.38	0.2	-0.034	1.8	-0.00190	-4.3

[a]Reference 47.

[b]Reference 33.

Table 10. Calculated and Experimental s_{33}^{sc} Coefficients and d_{33} Constants of Semicrystalline PVDF and 75 mol% P(VDF-TrFE)

Polymer	X_c	s_{33}^{sc}, m^2/N ($x10^{-10}$)	d_{33} [d a], pC/N	d_{33} (exp), pC/N
PVDF	0.1	8.29	-10.5	-32 [b]
	0.3	6.50	-24.8	
	0.5	4.72 [b]	-29.9	
	0.75	2.49	-23.7	
	0.9	1.15	-13.1	
75 mol% P(VDF-TrFE) (no local-field correction)	0.1	9.77	-10.4	-34.1 [b]
	0.3	7.69	-24.5	
	0.5	5.60	-29.7	
	0.75	3.0 [c]	-23.9	
	0.9	1.44	-13.7	
75 mol% P(VDF-TrFE) (local-field correction)[d]	0.1	9.77	-12.0	-34.1[b]
	0.3	7.69	-28.5	
	0.5	5.60	-34.5	
	0.75	3.0	-27.8	
	0.9	1.44	-16.0	

[a] $\theta = 0.95$ from reference 48.

[b] Reference 49.

[c] Reference 16.

[d] Correction estimated from Figure 3 in reference 43.

REFERENCES

1. R. G. Kepler, "Piezoelectricity, Pyroelectricity, and Ferroelectricity in Organic Materials," *Annual Review of Physical Chemistry*, vol. 29, 1978, p. 497.

2. R. G. Kepler and R. A. Anderson, "Ferroelectric Polymers," *Advances in Physics*, vol. 41, 1992, p. 1.

3. D. A. Summa, "Elastic and Dielectric Losses in Piezoelectric PVDF, P(VDF TrFE) Copolymer, and Selected Passive Polymers and Their Effect on Acoustic Performance of Broadband Transducers," Technical Report, Applied Research Laboratories, 18 June 1993.

4. J. Powers, "Long Range Hydrophones," in *The Applications of Ferroelectric Polymers*, T. T. Wang, J. M. Herbert, and A. M. Glass, eds., Chapman and Hall, New York, NY, 1988.

5. G. J. Kavarnos and E. A. McLaughlin, "Development of a High-Frequency Multilayer Copolymer Acoustic Projector," NUWC-NPT Technical Report 10,607, Naval Undersea Warfare Center Division, Newport, Rhode Island, 31 March 1994.

6. R. A. Ferren, "Synthesis of Poly(vinylidene Fluoride) and Its Copolymers," in *The Applications of Ferroelectric Polymers*, T. T. Wang, J. M. Herbert, and A. M. Glass, eds., Blackie, Glasgow, 1988, Chapter 2.

7. P. J. Flory, *Statistical Mechanics of Chain Molecules*, Hanser, Munich, 1989.

8. A. J. Lovinger, "Ferroelectric Polymers," *Science*, vol. 220, 1983, p. 1115.

9. A. J. Lovinger, "Poly(vinylidene Fluoride)," in *Developments in Crystalline Polymers – 1*, D. C. Bassett, ed., Applied Science, London, 1982, Chapter 5.

10. K. Koga, N. Nakano, T. Hattori, and H. Ohigashi, "Crystallization, Field-Induced Phase Transformation, Thermally Induced Phase Transition, and Piezoelectric Activity in P(Vinylidene fluoride-TrFE) Copolymers with High Molar Content of Vinylidene Fluoride," *Journal of Applied Physics*, vol. 67, 1990, p. 965.

11. R. J. Young and P. A. Lovell, *Introduction to Polymers*, 2nd ed., Chapman and Hall, London, 1991, p. 283.

12. L. Mandelkern, "The Structure of Crystalline Polymers," *Accounts of Chemical Research*, vol. 23, 1990, p. 380.

13. W. W. Doll and J. B. Lando, "Polymorphism of Poly(vinylidene Fluoride). III. The Crystal Structure of Phase II," *Journal of Macromolecular Science – Physics*, vol. B4, 1970, p. 309.

14. K. Tashiro, K. Takano, M. Kobayashi, Y. Chatani, and H. Tadokoro, "Structural Study on Ferroelectric Phase Transition of Vinylidene Fluoride-Trifluoroethylene Copolymers (III) Dependence of Transitional Behavior of VDF Molar Content," *Ferroelectrics*, vol. 57, 1984, p. 297.

15. R. A. Sorensen, W. B. Liau, and R. H. Boyd, "Prediction of Polymer Crystal Structures and Properties. A Method Utilizing Simultaneous *Inter*– and *Intra*molecular Energy Minimization," *Macromolecules*, vol. 21, p. 194.

16. H. Wang, Q. M. Zhang, and L. E. Cross, "Piezoelectric, Dielectric, and Elastic Properties of P(VDF/TrFE) Copolymer," *Journal of Applied Physics*, vol. 74, 1993, p. 3394.

17. R. J. Roe, ed., *Computer Simulation of Polymers*, Prentice-Hall, Englewood Cliffs, N. J., 1991.

18. J. Bicerano, "Force Field Calculations on Model Molecules Simulating Isolated Chain Segments of Poly(vinylidene halide) and Vinylidene Halide/Vinyl Halide Copolymers," *Macromolecules*, vol. 22, 1989, p. 1408.

19. C. R. A. Catlow, S. C. Parker, and M. P. Allen, eds., *Computer Modelling of Fluids, Polymers, and Solids*, NATO ASI Series, Kluwer, Dordrecht, 1990.

20. R. L. McCullough, "An Energetics Approach to the Analysis of Molecular Motions in Polymeric Solids," *Journal of Macromolecular Science – Physics*, vol. B9, 1974, p. 97.

21. N. L. Allinger, "Calculation of Molecular Structure and Energy by Force-Field Methods," *Advances in Physical Organic Chemistry*, vol. 13, 1976, p. 1.

22. A. Y. Meyer, N. L. Allinger, and Y. Yuh, "Updating the Molecular-Mechanical Force Field for Organic Halides," *Israel Journal of Chemistry*, vol. 20, 1980, p. 57.

23. U. Burkert and N. Allinger, *Molecular Mechanics*, American Chemical Society, Washington, DC, 1982.

24. W. J. Hehre, L. Radom, P. v.R. Schleyer, and J. A. Pople, *Ab Initio Molecular Orbital Theory*, Wiley, New York, 1986.

25. T. Clark, *A Handbook of Computational Chemistry*, Wiley, New York, 1985, pp. 12-92.

26. K. B. Lipkowitz, "MM2 Parameters," *QCPE Bulletin*, vol. XII, 1992, p. 6.

27. J. P. Bowen and N. L. Allinger, "Molecular Mechanics: The Art and Science of Parameterization," *Review of Computational Chemistry*, vol. 2, 1991, p. 81.

28. L. I. Schiff, *Quantum Mechanics*, McGraw-Hill, New York, 1968.

29. I. N. Levine, *Quantum Chemistry*, 4th ed., Prentice-Hall, Englewood Cliffs, N. J., 1991.

30. A. Hinchliffe, *Computational Quantum Chemistry*, Wiley, New York, 1988.

31. J. J. P. Stewart, "MOPAC: A Semiempirical Molecular Orbital Program," ***Journal of Computer-Aided Molecular Design***, vol. 4, 1990, p. 1.

32. M. Takakubo and K. Teramura, "Molecular Orbital Calculations of Poly(vinylidene Fluoride) and Its Model Compounds," ***Journal of Polymer Science: Part A: Polymer Chemistry***, vol. 27, 1989, p. 1897.

33. K. Tashiro, M. Kobayashi, H. Tadokoro, and E. Fukada, "Calculations of Elastic and Piezoelectric Constants of Polymer Crystalls by a Point Charge Model: Application to Poly(vinylidene fluoride) Form I," ***Macromolecules***, vol. 13, 1980, p. 691.

34. R. Hasegawa, Y. Takahashi, Y. Chatani, H. Tadakoro, "Crystal Structures of Three Crystalline forms of Poly(vinylidene fluoride)," ***Polymer Journal***, vol. 3, 1972, p. 600.

35. B. L. Farmer, A. J. Hopfinger, J. B. Lando, "Polymorphism of Poly(vinylidene fluoride): Potential Energy Calculations of the Effects of Head-to-Head Units on the Chain Conformation and Packing of Poly(vinylidene fluoride)," ***Journal of Appied Physics***, vol. 43, 1972, p. 4293.

36. R. Hasegawa, M. Kobayashi, and H. Tadakoro, "Molecular Conformation and Packing of Poly(vinylidene fluoride). Stability of Three Crystalline Forms and the Effect of High Pressure," ***Polymer Journal***, vol. 3, 1972, p. 591.

37. R. W. Holman and G. J. Kavarnos, "A Molecular Dynamics Investigation of the Structural Characteristic of Amorphous and Annealed Poly(vinylidene fluoride) and Vinylidene fluoride-trifluoroethylene Copolymers," NUWC-NPT Technical Report (in preparation), Naval Undersea Warfare Center Detachment, New London, CT.

38. A. J. Lovinger, T. Furukawa, G. T. Davis, and M. G. Broadhurst, "Crystallographic Changes Characterizing the Curie Transition in Three Ferroelectric Copolymers of Vinylidene Fluoride and Trifluoroethylene: 2. Oriented or Poled Samples," ***Polymer***, vol. 24, 1983, p. 1123.

39. H. Tanaka , H. Yukawa, and T. Nishi, "Effect of Crystallization Condition on the Ferroelectric Phase Transition in Vinylidene Fluoride/Trifluoroethylene (VF_2/F_3E) Copolymers," ***Macromolecules***, vol. 21, 1988, p. 2469.

40. H. E. Klei and J. J. Stewart, "Calculation of Polymer Elastic Moduli Using Semiempirical Methods," ***International Journal of Quantum Chemistry, Quantum Chemistry Symposium***, vol. 20, 1986, p. 529.

41. K. Tashiro, M. Kobayashi, and H. Tadokoro, ***Macromolecules***, vol. 11, 1978, p. 908.

42. J. J. P. Stewart, "MNDO Cluster Model Calculations on Organic Polymers," *New Polymeric Materials*, vol. 1, 1987, p. 53.

43. H. Ogura and A. Chiba, "Calculation of the Equilibrium Polarization of Vinylidene Fluoride-Trifluooroethylene Copolymers Using the Iteration Method," *Ferroelectrics*, vol 7, 1987, p. 347.

44. Y. Tajitsu, H. Ogura, S. A. Chiba, and T. Furukawa, "Investigation of Switching Characteristics of Vinylidene Fluoride/Trifluoroethylene Copolymers in Relation to Their Structures," *Japanese Journal of Applied Physics*, vol. 103, 1987, p. 554.

45. K. Tashiro and H. Tadokoro, "Estimating the Limiting Values of the Macroscopic Piezoelectric Constants of Poly(vinylidene fluoride) Form I," *Macromolecules*, vol. 16, 1983, p. 961.

46. T. Furukawa, J. X. Wen, K. Suzuki, Y. Takashina, and M. Date, "Piezoelectricity and Pyroelectricity in Vinylidene Fluoride/Trifluoroethylene Copolymers," *Journal of Applied Physics*, vol. 56, 1984, p. 829.

47. N. Karasawa and W. A. Goddard, III, "Force Fields, Structures, and Properties of Poly(vinylidene fluoride) Crystals," *Macromolecules*, vol. 25, 1992, p. 7268.

48. W. L. Bongianni, "Effect of Crystallization and Anneal on Thin Films of Vinylidene Fluoride/Trifluoroethylene (VF_2/F_3E) Copolymers," *Ferroelectrics*, vol 103, 1990, p. 57.

49. H. Schewe, "Piezoelectricity of Uniaxially Oriented Poly(vinylidene fluoride)," *Ultrasonic Symposium, Proceedings*, vol. 1, 1982, p. 519.

50. R. Al-Jishi and P. L. Taylor, "Field Sums for Extended Dipoles in Ferroelectric Polymers," *Journal of Applied Physics*, vol. 57, 1985, p. 897.

51. R. Al -Jishi and P. L. Taylor, "Equilibrium Polarization and Piezoelectric and Pyroelectric Coefficients in Poly(vinylidene fluoride)," *Journal of Applied Physics*, vol. 57, 1985, p. 902.

52. A. Sen, J. I. Scheinbeim, and B. A. Newman, "The Effect of Plasticizer on the Polarization of Poly(vinylidene fluoride) films," *Journal of Applied Physics*, vol. 59, 1984, p. 2433.

INITIAL DISTRIBUTION LIST

Addressee	No. of Copies
Office of Naval Research (Dr. W. A. Smith, Code 332; Dr. K. J. Wynne, Code 1113)	2
Pennsylvania State University (Prof. L. E. Cross, Prof. Q. Zhang)	2
South Dakota State University (Prof. L. F. Brown)	1
Rutgers University (Prof. J. Scheinbeim, Prof. B. Newman)	2
Defense Technical Information Center	2